

1-6 Geochemical Survey

1-6-1 Soil geochemistry in A-area

1) Sampling

Soil geochemical survey was conducted in combination with geological mapping at the scale of 1:10,000. As chromite ore deposits in ultramafic rocks are the most important in this area, each sampling site along streams were predetermined in ultramafic rocks' area on the map.

Soil from B horizon had been taken from opposite banks at points above the highest water level of the stream. The heavy mineral sand was collected from 5 kilograms of soil by panning and checked the weight per 1 kilogram's soil. About 1 kilogram of soil samples from right and left banks was mixed for chemical analysis sample.

Collected soil samples were air-dried and screened with an 80 mesh sieve. About 100 g of -80 mesh fraction of each dried sample was taken and divided into halves. One half was used for chemical analyses in the PETROLAB in Philippines while the other half was used for analyses in Chemex Labs. Ltd. in Canada.

The location map of the soil samples is shown in PL. 2.

2) Pathfinder elements and chemical analyses.

Chromite deposits associated with ultramafic rocks are known to exist in this area. As these ore deposits are associated with ophiolite complexes, seven elements were selected as pathfinder elements because of the high possibility of concentration: platinum (Pt), palladium (Pd), gold (Au), nickel (Ni), chromium (Cr), iron (Fe) and cobalt (Co).

The elements of Ni, Cr, Fe and Co were analyzed in PETROLAB while Pt, Pd and Au analyses were done in Chemex Labs. Ltd.

The results of sampling conditions and the analyses are shown in Appendix 7.

3) Data analyses

The method of basic statistical analysis and principal components analysis were used in this

survey.

The combined data of A-area and B-area were used for data processing, and same statistic values and anomalous values were used for geochemical analysis in A-area and B-area, because both of areas are mainly underlain by the Mt. Beaufort Ultramafics.

There is no one-to-one correspondence between the weight of heavy mineral sand and chemical data of soil samples. The average weight of heavy mineral sand from right and left bank soil was used for the calculation of correlation coefficients and principal components analysis.

(i) Statistical analysis

It is known that normal and lognormal distribution models are of great importance in processing geochemical data. In particular, the distribution of minor elements in geochemistry shows close resemblance to that of the lognormal law as long as the accuracy of analyses is enough. Accordingly the logarithmic transformation of raw data was done before the data were analyzed. The raw values for Pt, Pd and Au have below-detection-limit. If the value of the raw data is below-detection-limit, half of the detection limit value is used in data processing.

The maximum value, minimum value, median, mean value(m) and standard deviation(σ) are shown in Table 4.

Table 4 Basic Statistic quantities of soil samples in area A and B

element	range	median	linear		logarithmic		
			mean	std. dev.	mean	10 ^{1/2} mean	std. dev.
Pt (ppb)	2.5 - 120	2.5	6.5	13.9	0.540	3.5	0.351
Pd (ppb)	1 - 120	4	8.7	13.5	0.613	4.1	0.527
Au (ppb)	1 - 130	1	2.2	5.3	0.153	1.4	0.308
Ni (ppm)	28 - 16100	2690	2773.3	1964.4	3.261	1823.3	0.509
Cr (ppm)	100 - 324000	14000	17121.7	18206.2	3.998	9948.9	0.576
Fe (%)	2.8 - 53.4	10.5	13.3	9.0	1.043	11.0	0.254
Co (ppm)	17 - 1900	236	277.2	208.6	2.309	203.7	0.368

Histogram and cumulative probability curve of each element are shown in Appendix 8. The class interval of the histogram is half of the standard deviation.

Correlation coefficients between these elements are shown in Table 5. The strong correlations are recognized with the relations of Pt-Pd, Ni-Cr, Ni-Fe, Ni-Co, Ni-HM (heavy mineral sand), Cr-Fe, Cr-Co, Cr-HM, Fe-Co, Fe-HM and Co-HM. The scatter diagrams are shown in Fig. 17.

(ii) Element content map

The content of each element is classed by mean value and standard deviation, and plotted on the element content map (Fig. 19 to Fig. 25). The contour map and raw values of each element are shown in PL. 5 to PL. 11.

Threshold for classifying background and anomalous values about Ni, Cr, Fe, Co and Pd is decided taking into consideration the cumulative probability curves, mean value (m) and standard deviation (σ). On the probability paper (Appendix 8), cumulative lognormal distribution forms a straight line. If a population contains a group of high anomalous values, this line is skewed to the high value area. This high values part indicates that the samples included in it are geochemically anomalous one. The cumulative frequency curves of Ni, Cr, Fe and Co skew near the point of $m+1.0\sigma$. The curve of Pd skews about 40 ppb. These points, therefore, are the thresholds of the positive anomalies.

The threshold of Pt and Au are decided by percentile method, because the resulting values of these elements contain many below-detection-limit values. The raw data of Au are 85 percents of below-detection-limit. About 5 percents' probability value is 35 ppm. The raw data of Au are 80 percent of below-detection-limit. About 5 percent probability value is 8 ppb. These values are used for threshold.

On the probability curve, the weight of heavy mineral sand per one kilogram soil is lognormal in distribution and probability curve does not skew. The value of $m+2\sigma$ (32 g) is used for threshold of the weight of heavy mineral sand.

(iii) Distribution of anomalous area

On the basis of the above-mentioned thresholds, anomalous values of each element are shown in element content map. The results are as follows:

Heavy mineral sand in soil: The anomaly areas are distributed in the north area of Tagburos, around Bacungan, the northeast part of A-area, and the area along west coast.

Pt: Generally the content of Pt is very low in A-area. The anomaly areas are distributed in the north area of Tagburos, the north to northwest part of Bacungan and the middle part of the Malinao River.

Pd: The anomaly areas are distributed in the north of Tagburos, the north to northwest of Bacungan and middle part of Malinao River.

Au: Generally the content of Au are very low. No significant anomaly areas were detected.

Ni: The anomaly areas are distributed in the north area of Bacungan and the area from Tagkawayan to Tagminatay along west coast.

Cr: The anomaly areas are distributed in the north area of Tagburos, the area around Bacungan, and the area along west coast.

Co: The anomaly areas are distributed in the north area of Bacungan and along west coast.

(iv) Principal components analysis

The aim of principal components analysis (PCA) is to represent the large number of elements in the original data by smaller number of "factor". The covariance matrix obtained from standardized $((\text{raw value} - \text{mean})/(\text{standard deviation}))$ data set is equal with correlation coefficients matrix. We have used the correlation matrix as initial matrix for this principal components analysis. The correlation matrix obtained from data set is shown in Table 6.

The eigenvalues above 1.0 are component 1 and 2, and these components explain 75 percent of information. According to the factor loading matrix, elements can be divided into 2 groups. Ni, Cr, Fe and Co have strong positive loading on component 1. Pt, Pd and Au have strong negative loading on component 2.

These results mean that the samples with high scores on component 1 are generally enriched in Ni, Cr, Fe and Co and the sample with negative scores on component 2 are enriched in Pt, Pd and Au compared with the other samples.

The scores calculated from weight vector are shown on scores distribution maps (Fig. 26 to Fig. 27). The cumulative probability plots of scores are shown in Appendix 9. The component 1 scores of more than $m+1\sigma$ and the component 2 scores of less than $m-\sigma$ area were picked up for anomaly.

The anomaly areas of component 1 are distributed in the north area of Tagbueros, the north area of Bacungan, and the area from Malinao River to Tagminatay. The anomaly areas of components 2 are almost overlapped with that of component 1.

4) Results of soil geochemistry

Interpretation map (Fig. 4) shows the anomaly areas of principal component 1 summarizing the content of Ni, Cr, Fe and Co, component 2 summarizing the content of Pt, Pd and Au, the anomaly areas of heavy mineral sand in soil, and the distribution of ultramafic rocks.

The promising areas overlapping with several anomaly areas are shown as follows:

1. The area on the north of Tagbueros
2. The area from the north of Bacungan to west coast
3. The area from Malinao River to Tagminatay

Table 5 Correlation coefficients of soil samples in area A and B

n = 984

	Pt	Pd	Au	Ni	Cr	Fe	Co	HM
Pt	1.000	0.566	0.317	0.157	0.205	0.381	0.271	0.209
Pd	0.566	1.000	0.399	0.182	0.239	0.270	0.252	0.214
Au	0.317	0.399	1.000	-0.082	-0.041	0.043	0.004	-0.014
Ni	0.157	0.182	-0.082	1.000	0.862	0.625	0.861	0.498
Cr	0.205	0.239	-0.041	0.862	1.000	0.540	0.774	0.678
Fe	0.381	0.270	0.043	0.625	0.540	1.000	0.855	0.456
Co	0.271	0.252	0.004	0.861	0.774	0.855	1.000	0.542
HM	0.209	0.214	-0.014	0.498	0.678	0.456	0.542	1.000

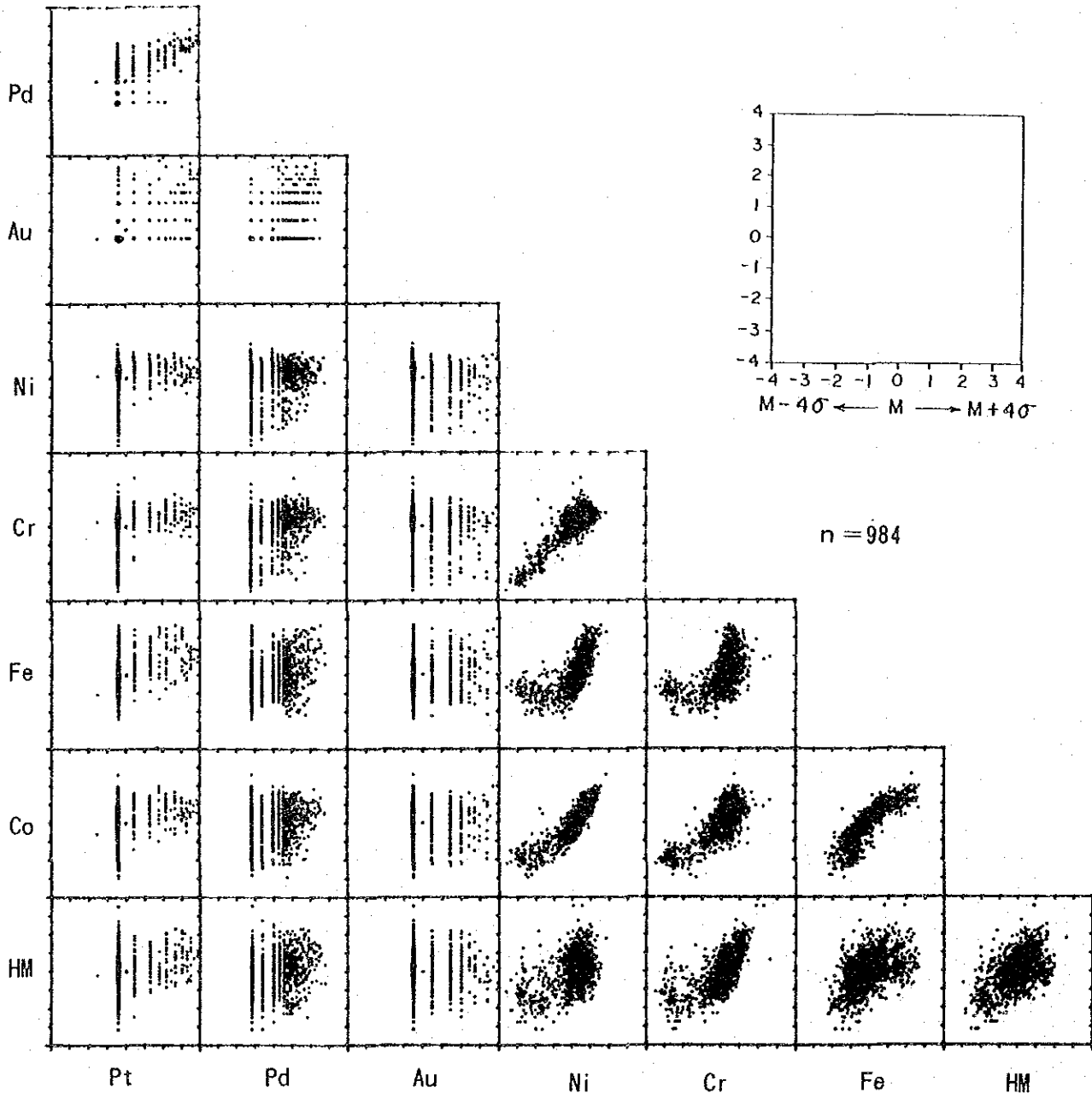
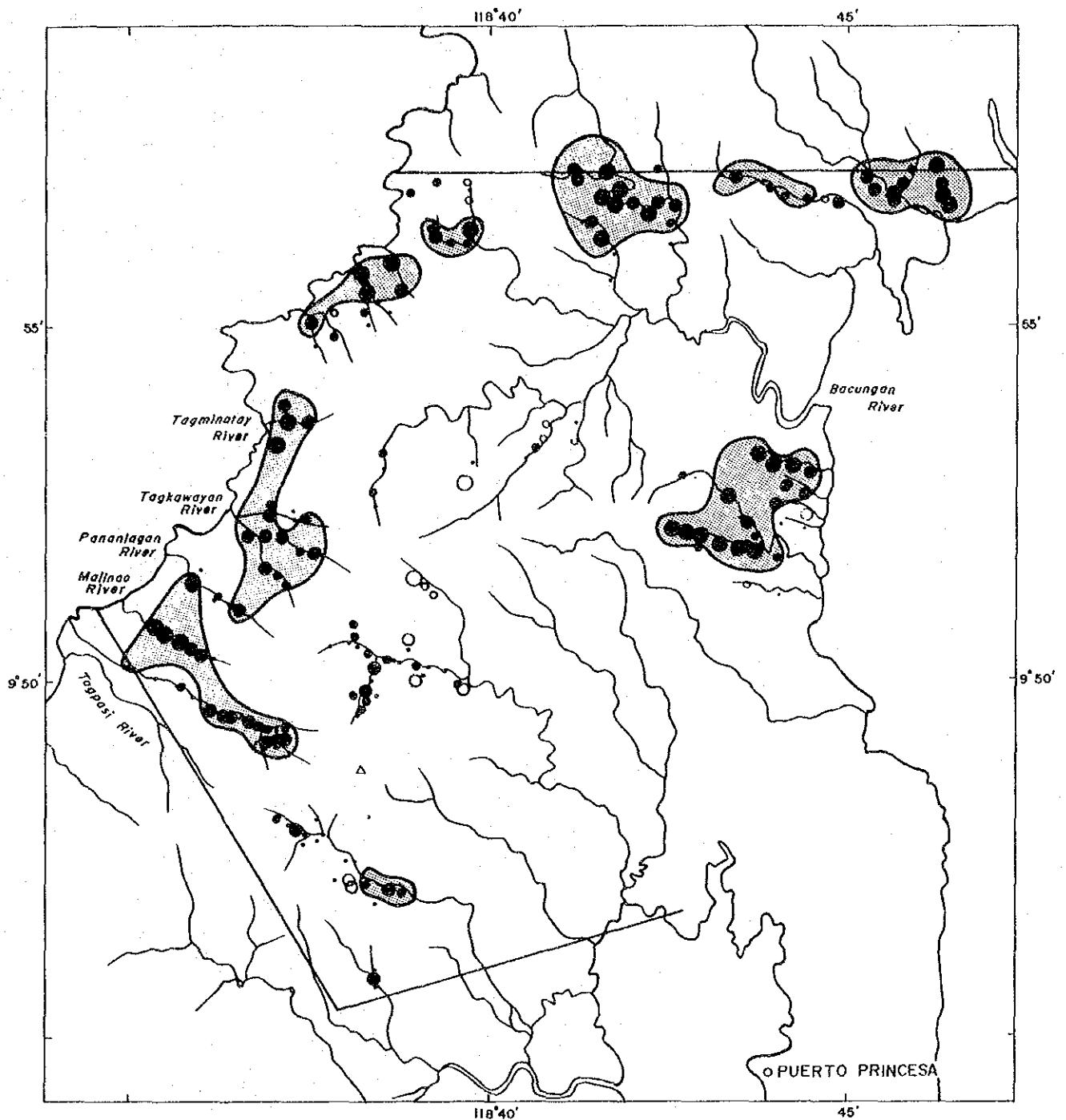


Fig. 17 Scatter diagram of soil samples in area A and B



LEGEND

●	29.8 ~ (g)
●	17.4 ~ 29.7
●	10.2 ~ 17.3
•	3.5 ~ 10.1
○	2.1 ~ 3.4
○	1.2 ~ 2.0
○	~ 1.2
● (shaded)	Anomaly area (32 ~)

Note : Plotted data from average weight of right and left bank samples. Anomaly areas are extracted from original data.

Fig.18 Heavy mineral content of soil samples in area A

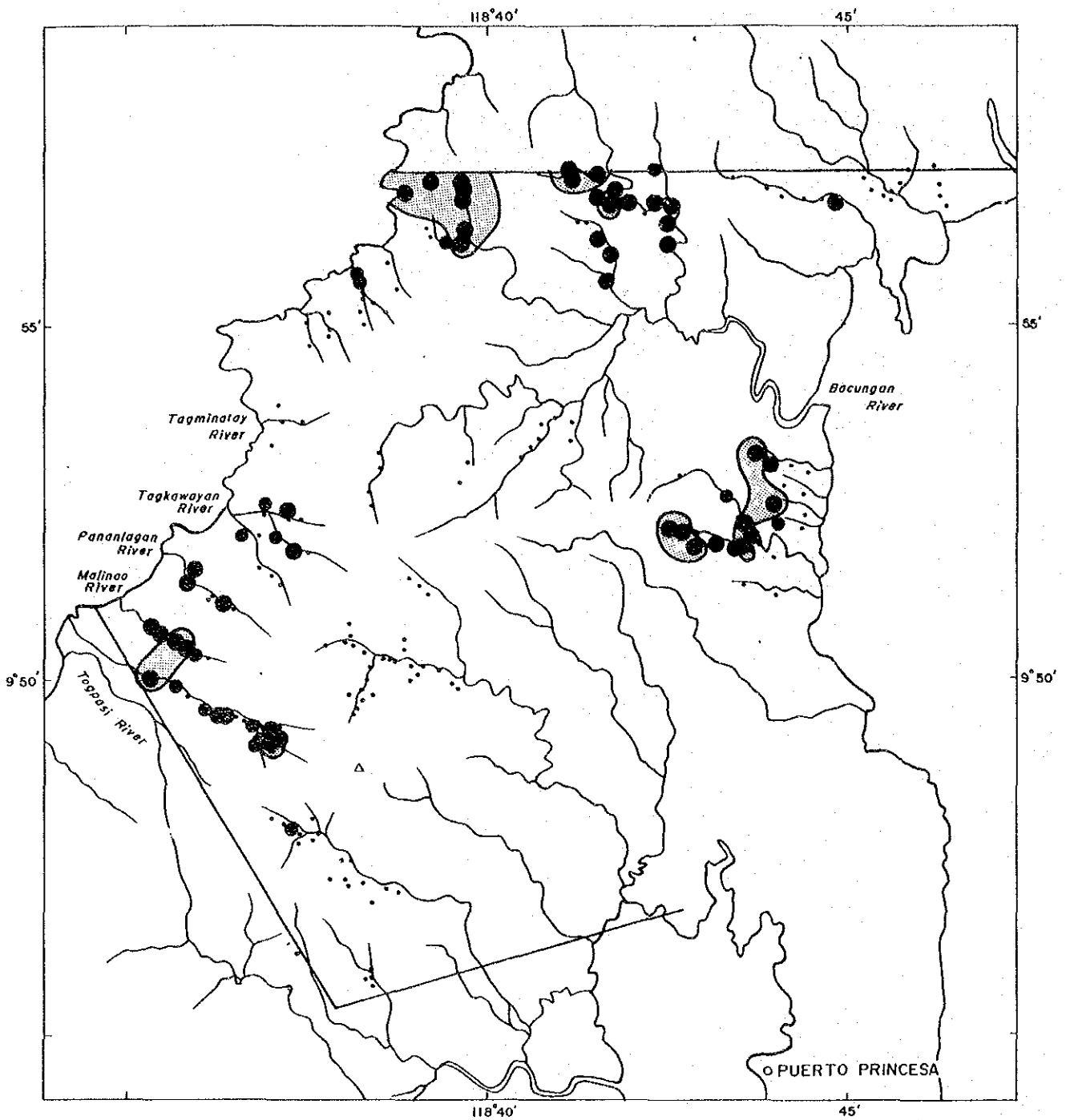
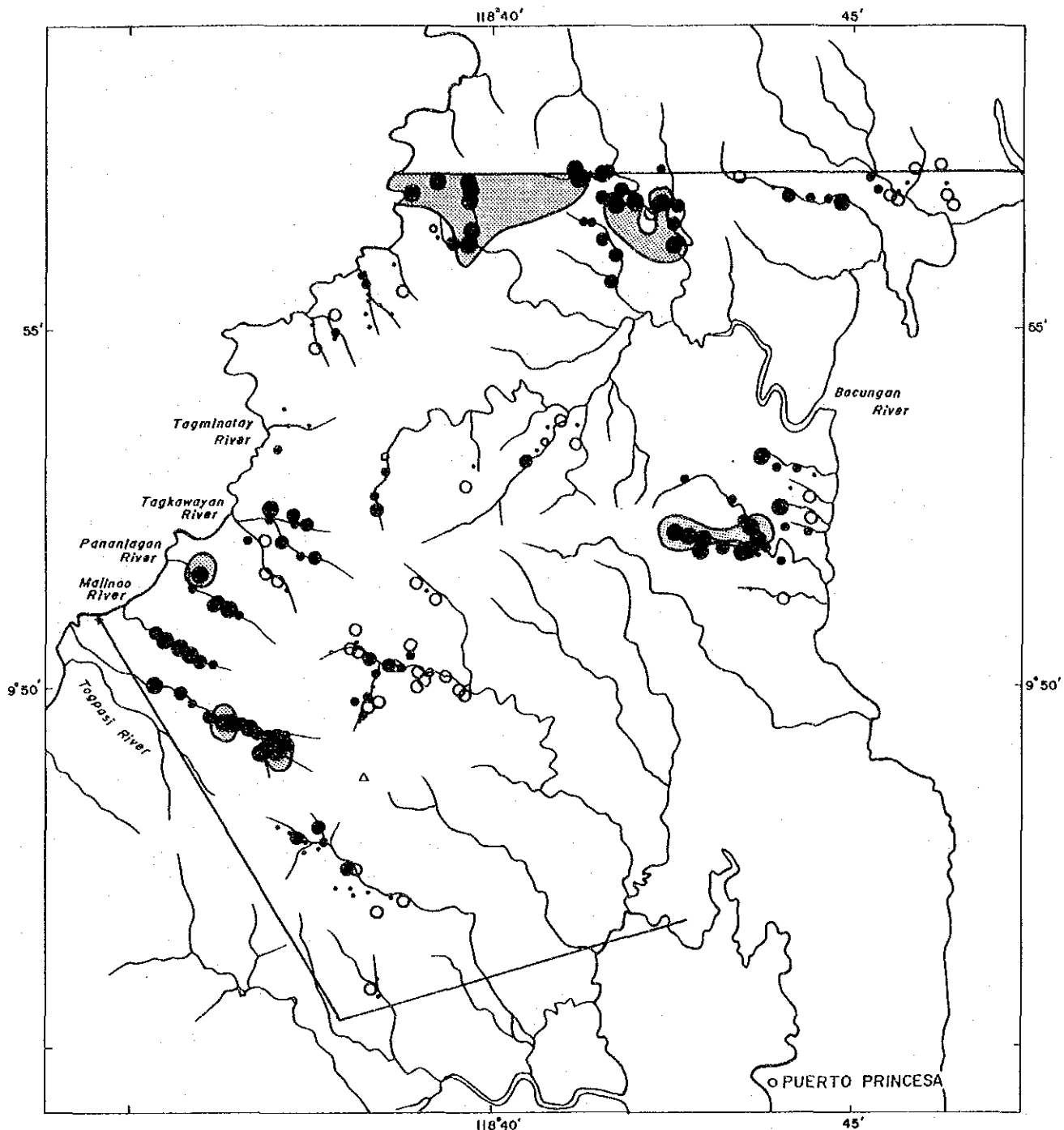


Fig. 19 Pt content of soil samples in area A



LEGEND

- 26 ~ (ppb)
- 14 ~ 24
- 8 ~ 12
- 4 ~ 6
- 2
- < 2
- Anomaly area (40~)

Fig. 20 Pd content of soil samples in area A

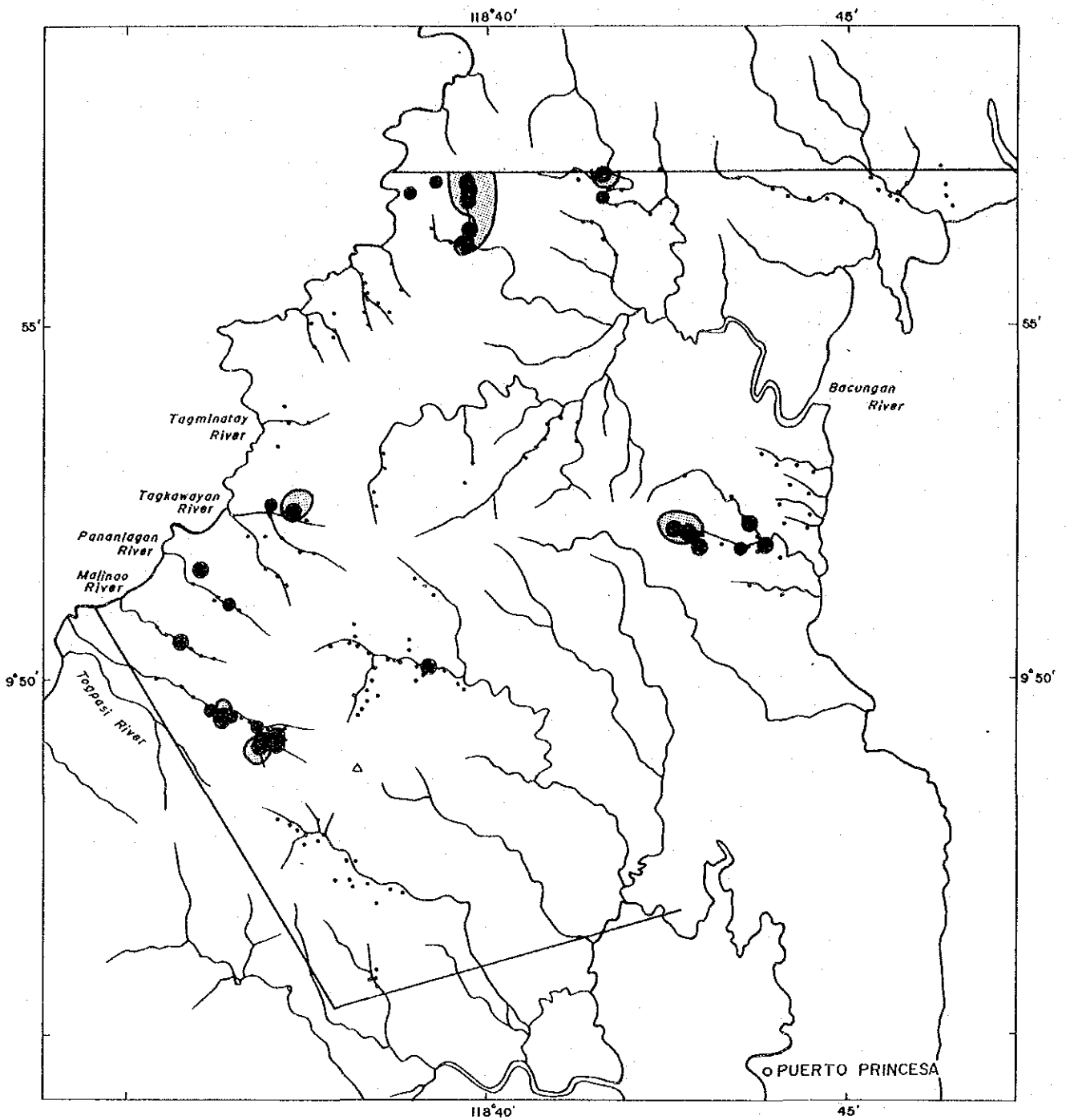
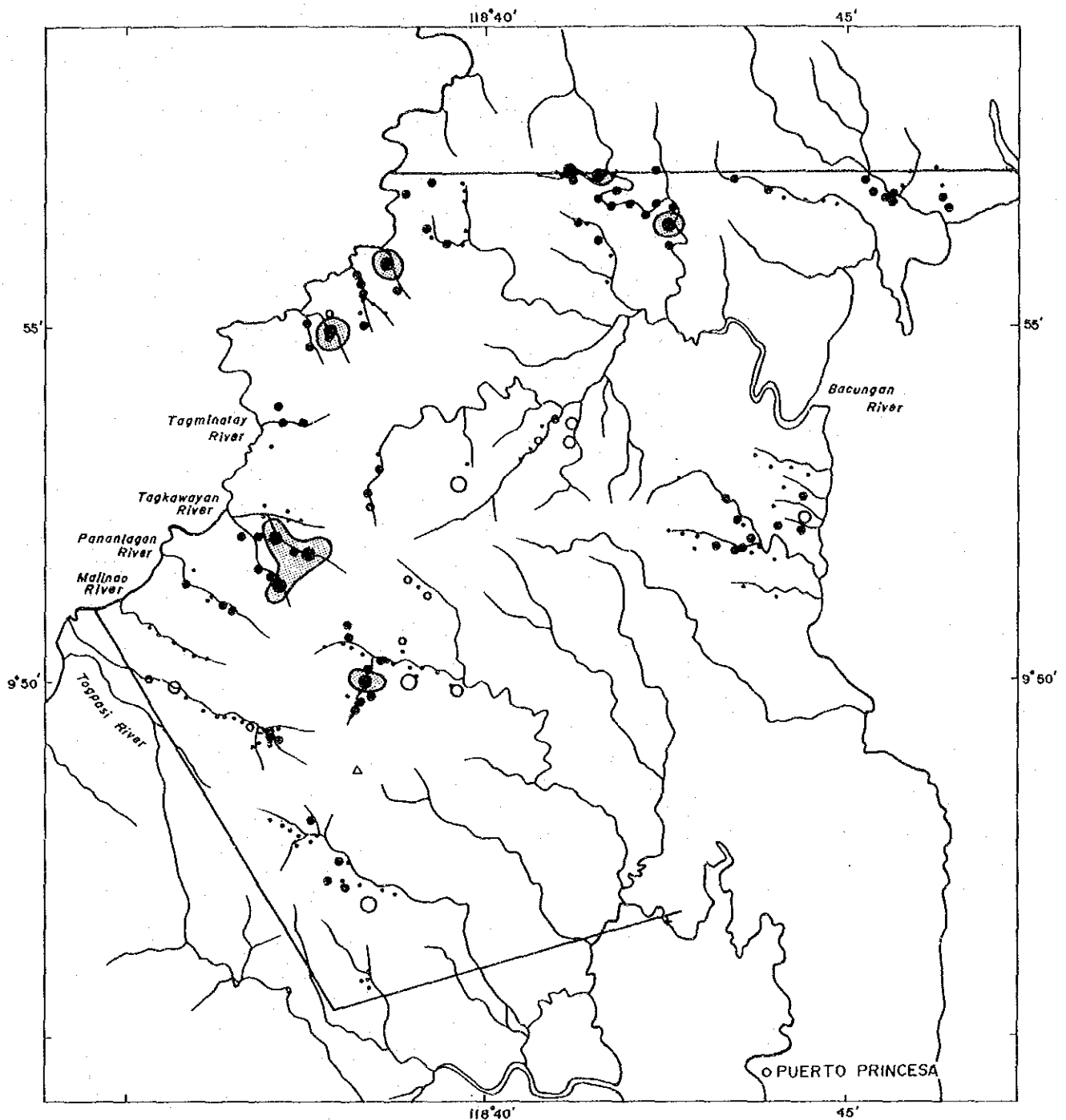


Fig.21 Au content of soil samples in area A

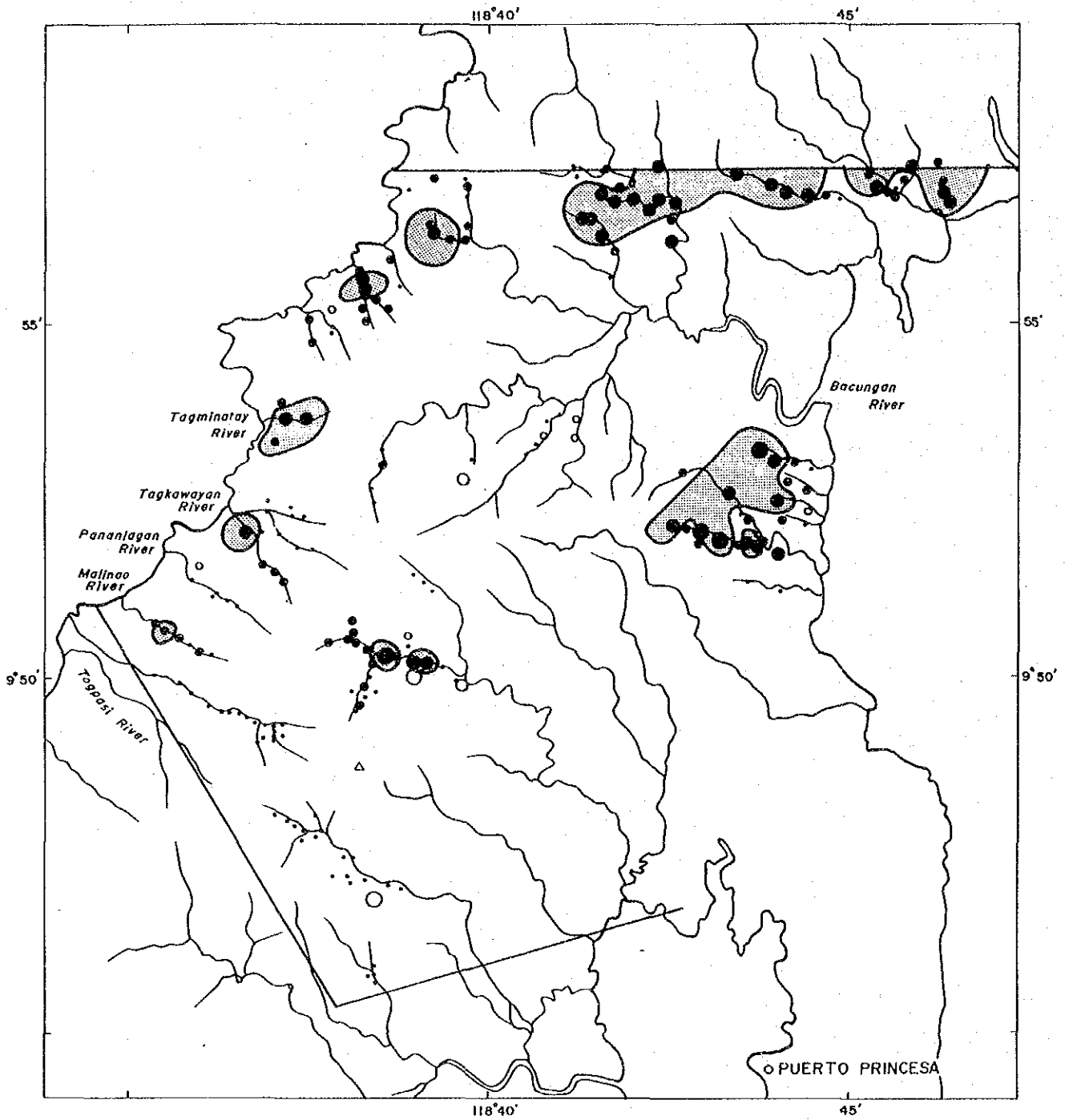


LEGEND

- 5890 ~ (ppm)
- 3280 ~ 5880
- 1020 ~ 3270
- 560 ~ 1010
- 320 ~ 550
- ~ 310
- ◐ Anomaly area (5888 ~)

0 5 km

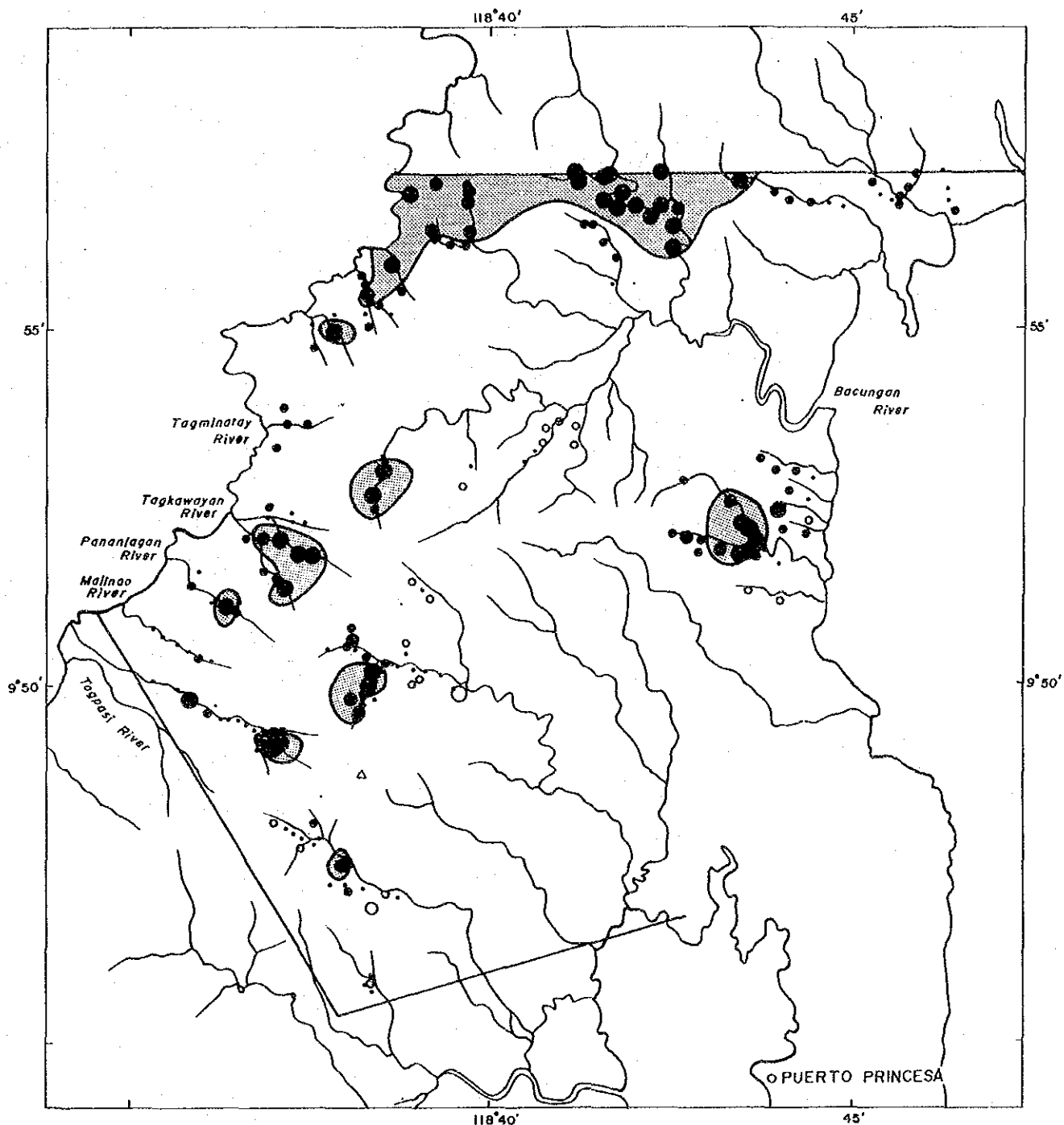
Fig. 22 Ni content of soil samples in area A



LEGEND

- 7.3 ~ (%)
- 3.8 ~ 7.2
- 2.0 ~ 3.7
- 0.52 ~ 1.9
- 0.27 ~ 0.51
- 0.41 ~ 0.26
- ~ 0.13
- Anomaly area (3.7 ~)

Fig. 23 Cr content of soil samples in area A



LEGEND

- 26.6 ~ (%)
- 19.9 ~ 26.5
- 14.8 ~ 19.8
- 8.3 ~ 14.7
- 6.2 ~ 8.2
- 4.6 ~ 6.1
- ~ 4.5
- Anomaly area (26.5 ~)

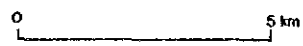
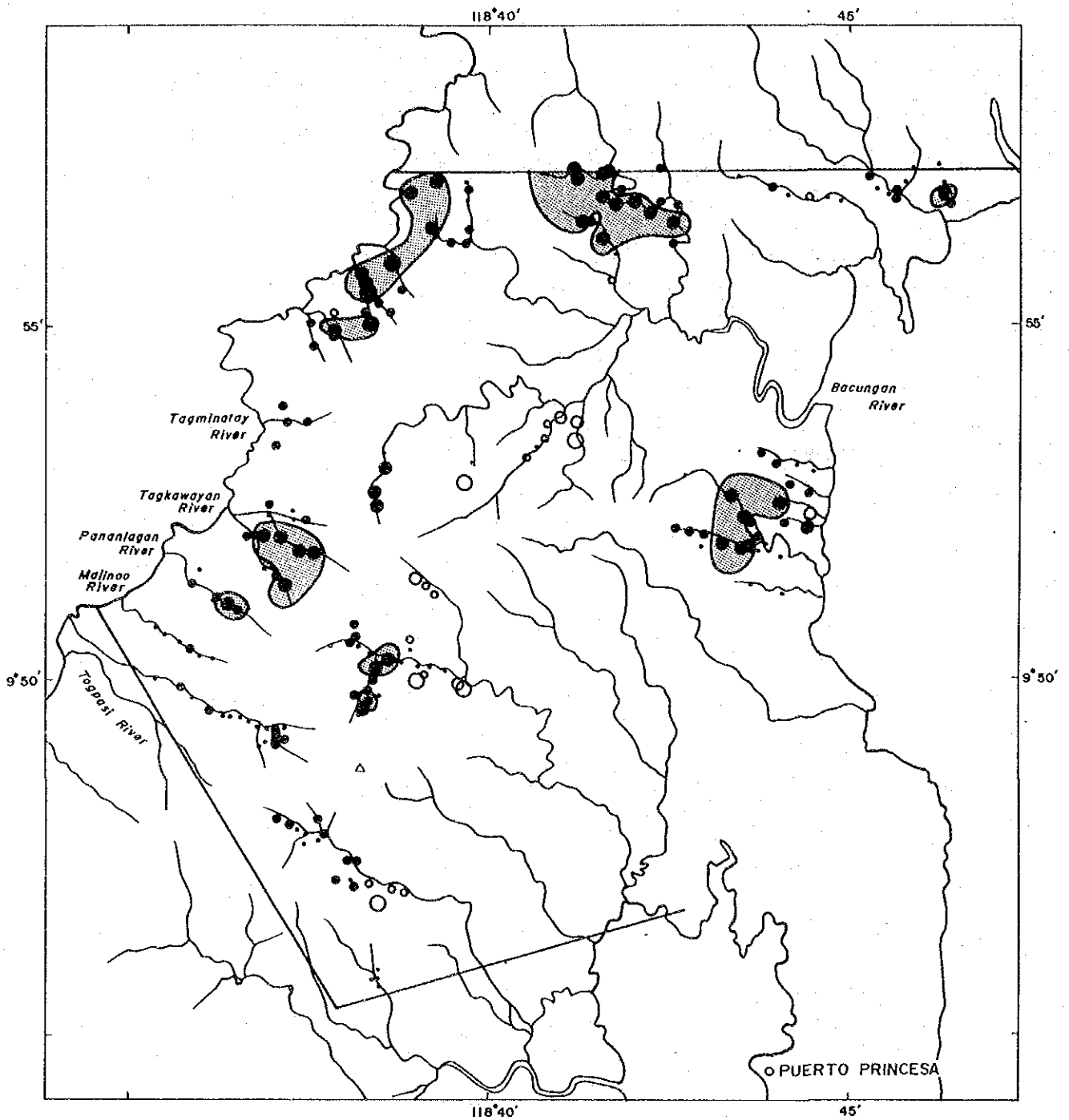


Fig.24 Fe content of soil samples in area A



LEGEND

- 730 ~ (ppm)
- 480 ~ 720
- 320 ~ 470
- 140 ~ 310
- 88 ~ 130
- 58 ~ 87
- ~ 57
- Anomaly area (480~)

Fig. 25 Co content of soil samples in area A

Table 6

Results of principal components analysis in area A and B

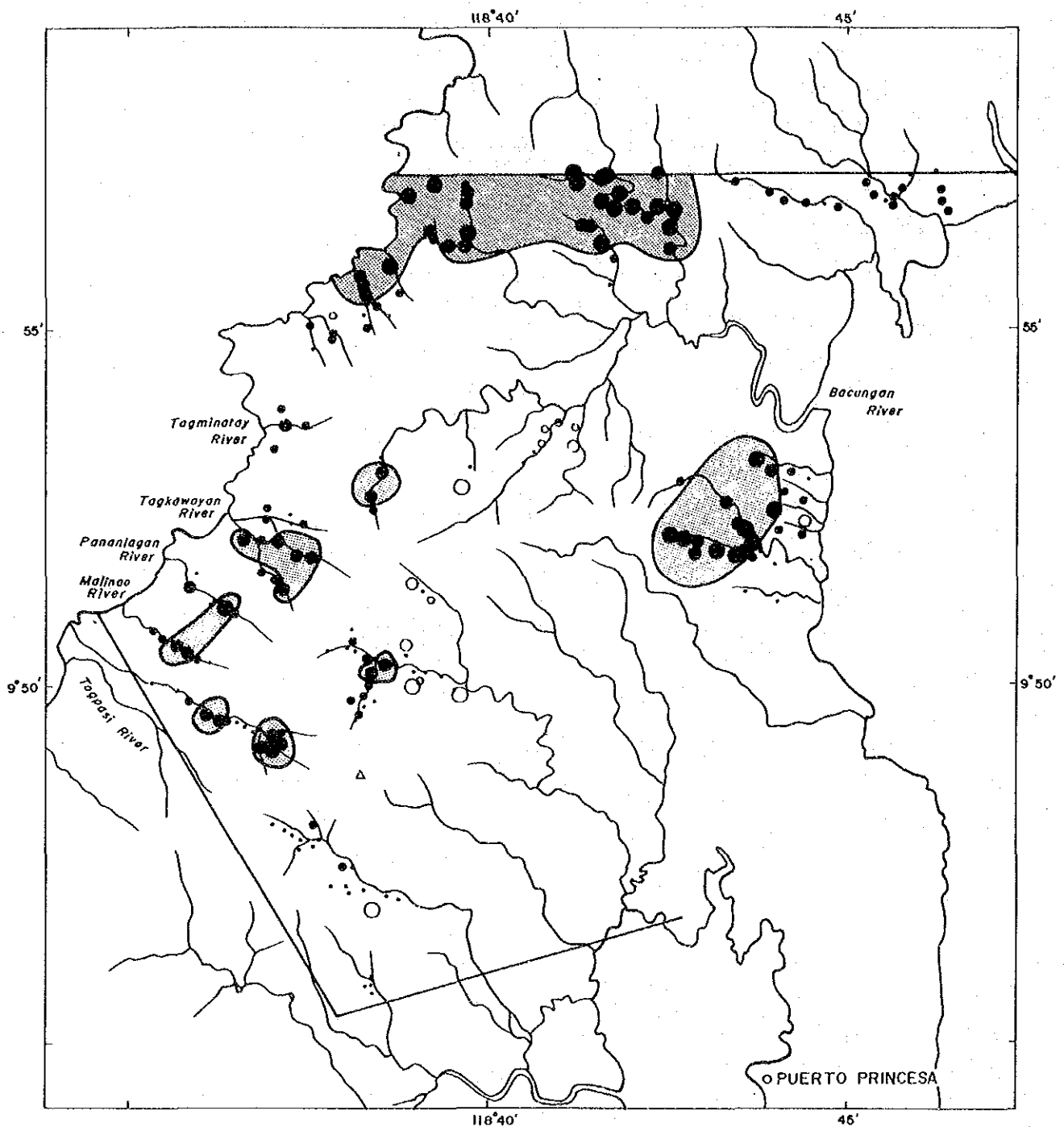
COMPONENT	EIGENVALUE	PERCENT	CUMULATIVE
Z-01	<u>3.9467</u>	49.3356	49.3356
Z-02	<u>1.7180</u>	21.4762	70.8118
Z-03	0.6806	8.5074	79.3193
Z-04	0.6483	8.1046	87.4239
Z-05	0.4868	6.0857	93.5096
Z-06	0.3681	4.6012	98.1107
Z-07	0.0936	1.1701	99.2808
Z-08	0.0575	0.7192	100.0000
TOTAL	8.0000	100	

Factor Loading

	Z-01	Z-02	Z-03	Z-04	Z-05	Z-06	Z-07	Z-08
Pt	0.4393	<u>-0.6834</u>	0.3239	0.2946	0.1521	0.3525	-0.0202	-0.0098
Pd	0.4261	<u>-0.7212</u>	-0.0320	0.2198	-0.3912	-0.3098	-0.0023	0.0028
Au	0.0786	<u>-0.7499</u>	-0.3892	-0.5053	0.1423	0.0670	-0.0023	0.0074
Ni	<u>0.8697</u>	0.2839	-0.0168	-0.1606	-0.2624	0.1679	-0.1690	0.1068
Cr	<u>0.8761</u>	0.2239	-0.2505	0.0533	-0.1740	0.1956	0.2191	-0.0056
Fe	<u>0.8216</u>	-0.0052	0.3767	-0.1958	0.2630	-0.2399	0.0874	0.1021
Co	<u>0.9301</u>	0.1523	0.1505	-0.2143	0.0062	-0.0663	-0.0574	-0.1883
Heavy Min.	<u>0.7085</u>	0.1214	-0.4422	0.3808	0.3493	-0.1224	-0.0754	0.0082

Eigen Vector

	Z-01	Z-02	Z-03	Z-04	Z-05	Z-06	Z-07	Z-08
Pt	0.2211	-0.5214	0.3926	0.3659	0.2181	0.5811	-0.0661	-0.0408
Pd	0.2145	-0.5502	-0.0388	0.2730	-0.5607	-0.5106	-0.0076	0.0115
Au	0.0396	-0.5721	-0.4718	-0.6275	0.2039	0.1104	-0.0076	0.0309
Ni	0.4378	0.2166	-0.0204	-0.1994	-0.3761	0.2767	-0.5523	0.4453
Cr	0.4410	0.1708	-0.3037	0.0662	-0.2494	0.3224	0.7163	-0.0235
Fe	0.4135	-0.0040	0.4566	-0.2432	0.3770	-0.3954	0.2856	0.4258
Co	0.4682	0.1162	0.1824	-0.2662	0.0088	-0.1093	-0.1875	-0.7848
Heavy Min.	0.3566	0.0926	-0.5361	0.4729	0.5006	-0.2017	-0.2465	0.0341



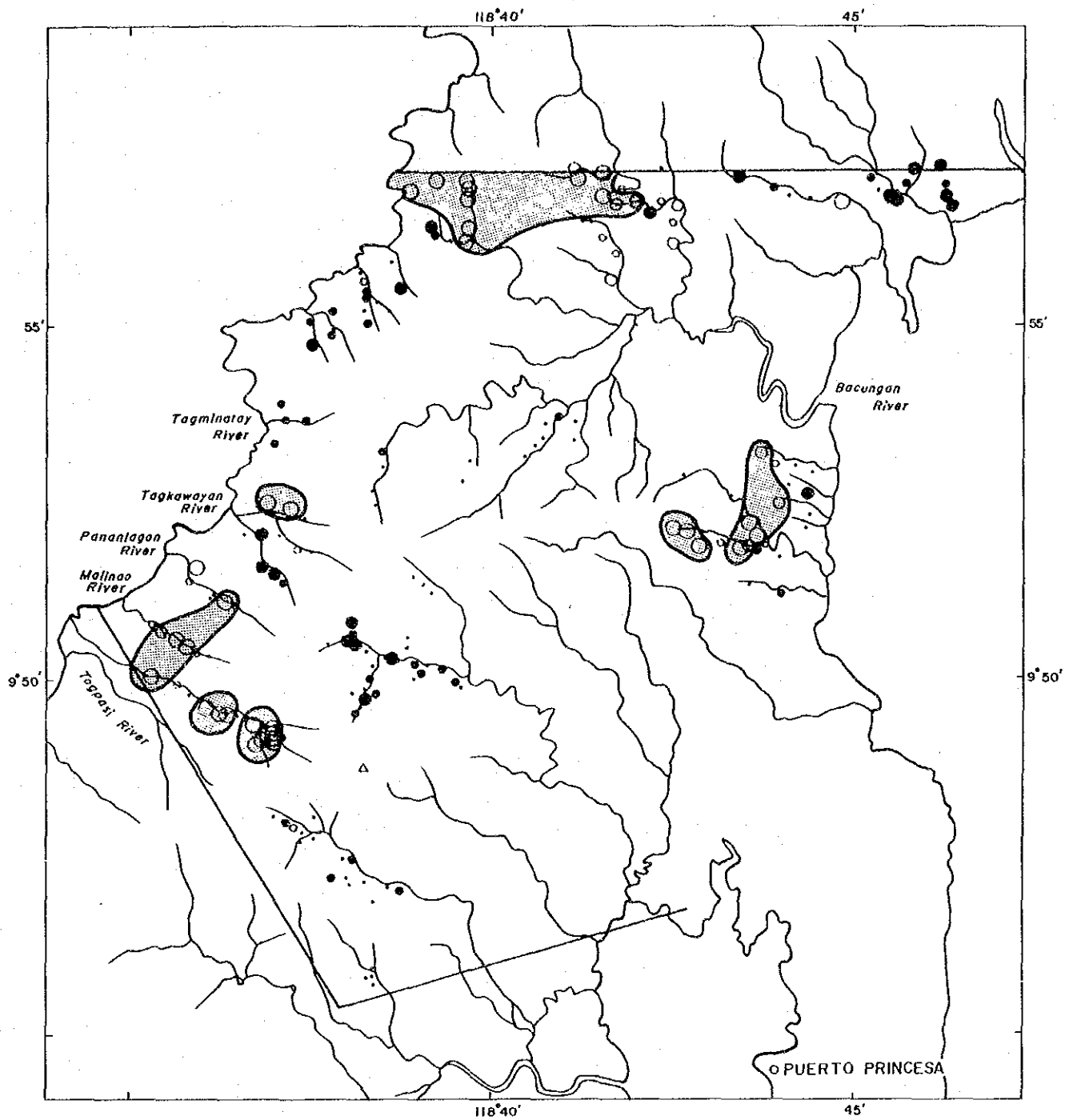
LEGEND

- 2.98 ~
- 1.98 ~ 2.98
- 0.99 ~ 1.98
- -0.99 ~ 0.99
- -1.98 ~ -0.99
- -2.98 ~ -1.98
- ~ -2.98
- Anomaly area (1.98 ~)

0 5 km

Fig. 26

Scores of principal components analysis in area A (Z1)



LEGEND

- 1.97 ~
- 1.31 ~ 1.97
- 0.66 ~ 1.31
- -0.66 ~ 0.66
- -1.31 ~ -0.66
- -1.97 ~ -1.31
- ~ -1.97
- Anomaly area (~ -1.97)

0 5 km

Fig. 27

Scores of principal components analysis in area A (Z2)

1-6-2 Soil geochemistry in detailed survey area A-1

The A-1 anomalous area is the area from Malinao River to Tagminatay along the west coast, located in the west part of A-area. This area was followed up with detailed geologic mapping and close spaced soil sampling designed along spurs and ridges.

1) Sampling and chemical analysis

Soil geochemical survey was conducted in combination with geological mapping at a scale of 1:5,000. Sampling method in area A-1 was almost the same with that of A-area.

Soil from B horizon had been taken from opposite banks, and soil samples from each bank were treated and analyzed separately. Same elements as A-area were selected as pathfinder elements because of the high possibility of concentration: platinum (Pt), palladium (Pd), gold (Au), nickel (Ni), chromium (Cr), iron (Fe) and cobalt (Co).

The location map of the soil samples is shown in PL. 15. The results of sampling conditions and the analyses are shown in Appendix 10.

2) Data analyses

The method of basic statistical analysis and principal components analysis were used in this survey.

(i) Statistical analysis

The range, median, mean and standard deviation(σ) are shown in Table 7. Area A-1 is the anomaly area of A-area, so medians and mean values of all elements are higher than the values calculated from A-area and B-area data set.

Histogram and cumulative probability curve of each element are shown in Appendix 11. The class interval of the histogram is half of the standard deviation.

Correlation coefficients between these elements are shown in Table 8. The strong positive correlations more than +0.5 are recognized with the relations of Pt-Pd, Ni-Cr, Ni-Fe, Ni-Co, Cr-Co and Fe-Co. These results are almost the same with that from A-area and B-area data set. The scatter diagrams are shown in Fig. 28.

Table 7 Basic Statistic quantities of soil samples in area A-1

element	range	median	linear		logarithmic		
			mean	std. dev.	mean	10 ⁷ mean	std. dev.
Pt (ppb)	2.5 - 320	25	29.7	25.8	1.331	21.4	0.382
Pd (ppb)	1 - 650	12	18.2	25.1	1.067	11.7	0.421
Au (ppb)	1 - 270	1	4.5	12.0	0.314	2.1	0.447
Ni (ppm)	2 - 17200	3200	3657.7	2653.7	3.396	2489.8	0.485
Cr (ppm)	140 - 71000	19000	20336.2	11429.0	4.195	15669.2	0.403
Fe (%)	3.0 - 55.0	16.8	18.0	7.9	1.212	16.3	0.199
Co (ppm)	4 - 1890	390	453.9	271.0	2.557	361.0	0.343

(ii) Element content map

The content of each sample is classed by mean value and standard deviation, and plotted on the element content map (Fig. 29 to Fig. 35). The contour map and raw values of each element are shown in PL. 17 to PL. 23. These maps show which bank the sample was taken.

Area A-1 is one of the anomaly areas in A-area, therefore we can't apply the same threshold with A-area and B-area to this area A-1. New threshold for area A-1 is considered mean value (m) and standard deviation (σ), and the point of $m+1.0\sigma$ was adopted as threshold.

On the basis of the above-mentioned thresholds, anomalous values of each element are shown in element content map. The results are as follows:

Pt: The anomaly areas are distributed in the upper stream of Malinao River, the area along Pananlagan River, and the area around Tagkawayan mineral showing.

Pd: The anomaly areas are distributed in the upper stream of Malinao River, the lower stream of Pinamunoan River, the area along the Pananlagan River, and the area on the south of the Tagminatay.

Au: The anomaly areas are distributed in the upper stream of Malinao River, the lower stream of Pinamunoan River, the area around Pananlagan mineral showings, and the area on the south of Tagminatay.

Ni: The content in the northern half of area A-1 is higher than that of southern half. The high content areas are the area from the upper stream of Pananlagan River to the middle-upper stream of Tagkawayan, and the area in the north of Tagminatay.

Cr: The content in the northern half of area A-1 is higher than that of southern half. The anomaly areas are the middle of area A-1, and the area from Pananlagan to Tagkawayan. The anomaly area from Pananlagan to Tagkawayan is concerned with Pananlagan and Tagkawayan mineral showings. Though the rather high content area exists around Macasaet area, which are significant mineral showings in area A-1, no remarkable anomaly is obtained.

Fe: The content in the northern half of area A-1 is higher than that of southern half. Remarkable high content area was detected from Tagkawayan River to Tagminatay.

Co: The content in the southern half of area A-1 is low. The high content areas are distributed as follows; the area from Pananlagan mineral showings to the upper stream of Tagkawayan, and the south part of Tagminatay.

(iii) Principal components analysis

The aim of principal components analysis (PCA) is to represent the large number of elements in the original data by smaller number of "factor". The covariance matrix obtained from standardized ((raw value - mean)/(standard deviation)) data set is equal with correlation coefficients matrix. We have used the correlation matrix as initial matrix for this principal components analysis. The correlation matrix obtained from data set is shown in Table 9.

The eigenvalues above 1.0 are component 1 and 2, and these components explain 72 percent of information. According to the factor loading matrix, the elements can be divided into 2 groups. Ni, Cr, Fe and Co have strong positive loading on component 1. Pt, Pd and Au have strong positive loading on component 2.

These results mean that the samples with high scores on component 1 are generally enriched in Ni, Cr, Fe and Co and the sample with positive scores on component 2 are enriched in Pt, Pd and Au compared with the other samples.

The scores calculated from weight vector are shown on scores distribution maps (Fig. 36 to Fig. 37). The cumulative probability plots of scores are shown in Appendix 12. The component 1 scores of more than $m+1\sigma$ and the component 2 scores of more than $m+\sigma$ area were picked up

as anomalous area.

The high scores areas of component 1 are distributed in the area from the upper stream of Pananlagan River to the upper part of Tagkawayan and the area on the south of Tagminatay. These areas contain Pananlagan and Tagkawayan mineral showings. The anomalous areas of components 2 are distributed in the upper stream of Malinao River, the basin of Pananlagan River, the upper part of Pananlagan River and the area from Tagkawayan mineral showings to Tagmintay.

3) Results of soil geochemistry

Interpretation map (Fig. 5) shows the anomaly areas of principal component 1, which summarizes the content of Ni, Cr, Fe and Co, and component 2, which summarizes the content of Pt, Pd and Au, and the distribution of dunite. The promising areas overlapping with several anomaly are shown as follows:

1. The area around Pananlagan mineral showings
2. The area from Tagkawayan mineral showings to the southern part of Tagminatay

The high content of Fe in soil indicates the development of residual lateritic soil. Perhaps the high contents of Fe and Ni mean the distribution of nickel laterite. The upper stream of Tagkawayan and the north part of Tagminatay have the potential of nickel lateritic soil.

Table 8 Correlation coefficients of soil samples in area A-1

n=1371

	Pt	Pd	Au	Ni	Cr	Fe	Co
Pt	1.000	0.664	0.229	0.179	0.266	0.167	0.280
Pd	0.664	1.000	0.425	-0.078	0.043	0.013	0.007
Au	0.229	0.425	1.000	-0.124	-0.052	-0.124	-0.086
Ni	0.179	-0.078	-0.124	1.000	0.676	0.690	0.878
Cr	0.266	0.043	-0.052	0.676	1.000	0.336	0.655
Fe	0.167	0.013	-0.124	0.690	0.336	1.000	0.729
Co	0.280	0.007	-0.086	0.878	0.655	0.729	1.000

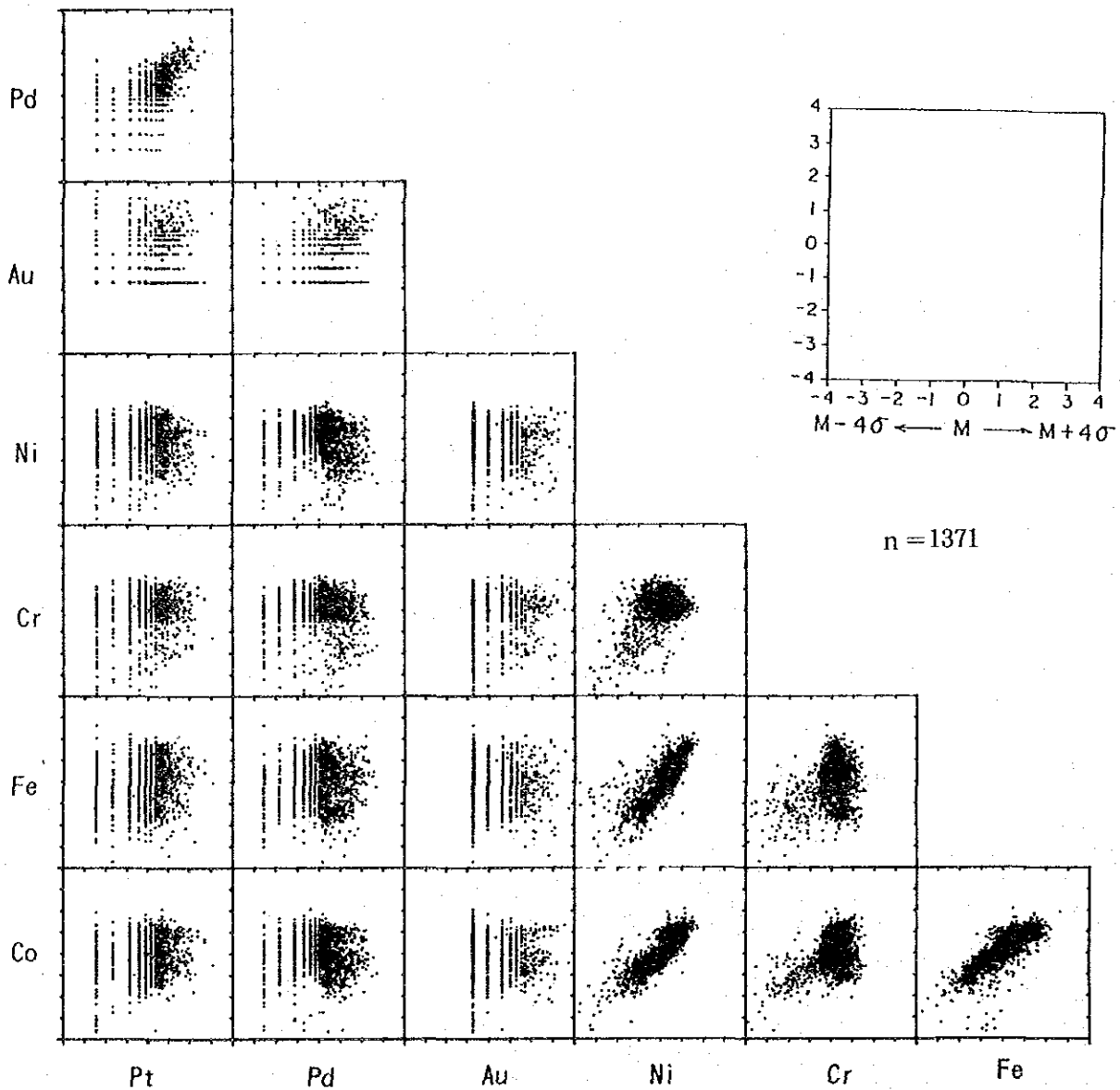


Fig. 28 Scatter diagram of soil samples in area A-1

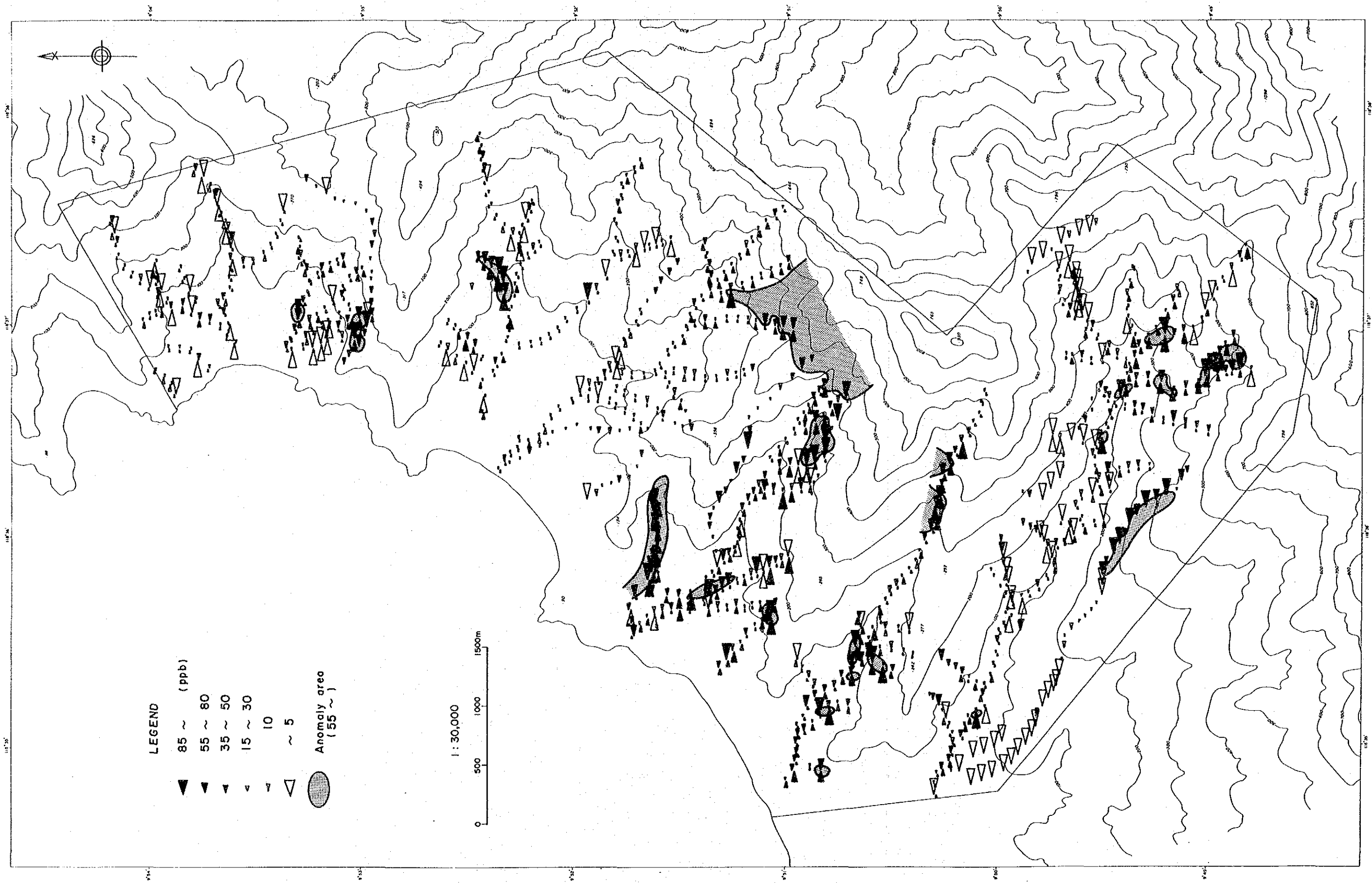


Fig.29 Pt content of soil samples in area A-1

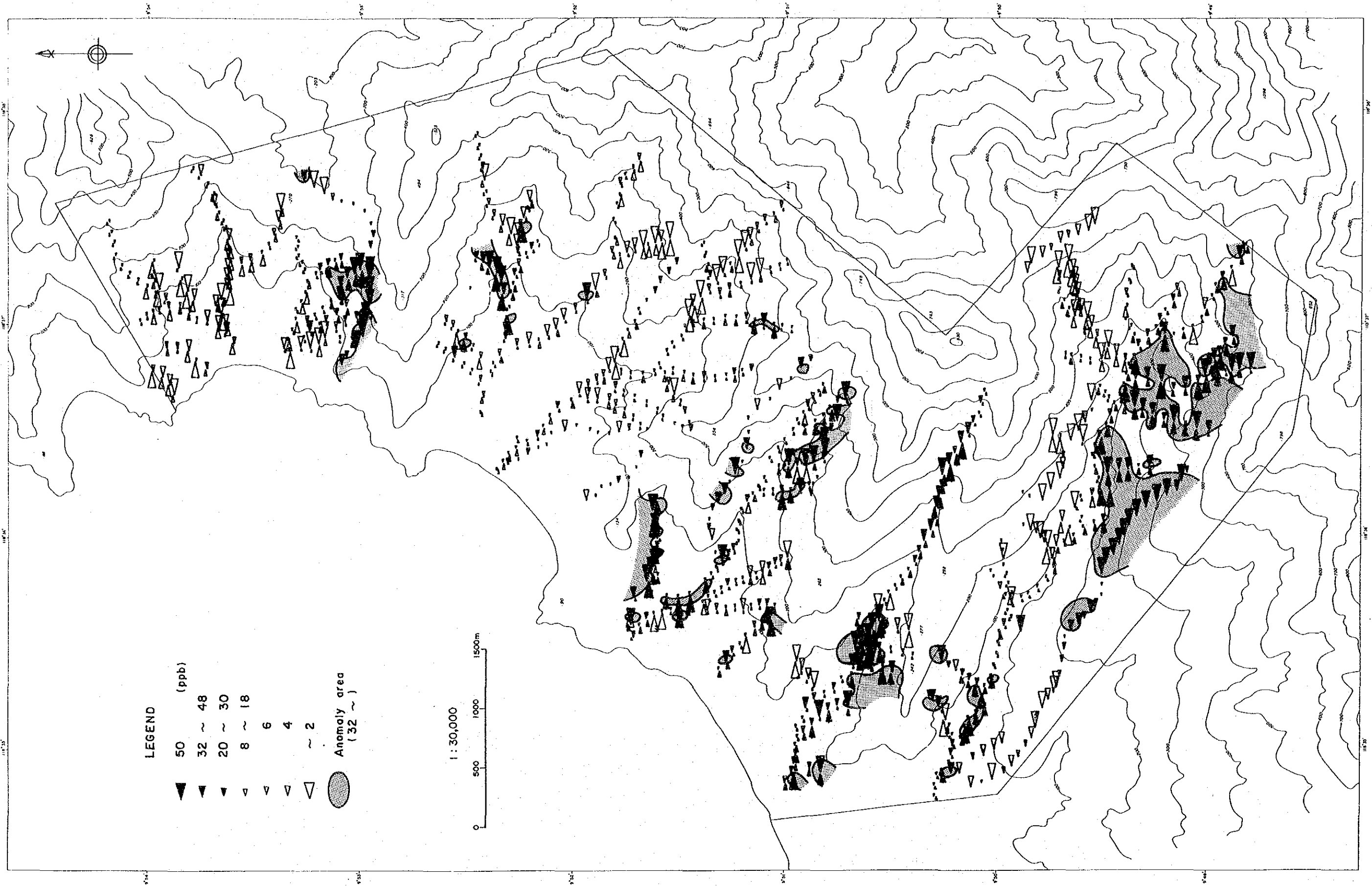


Fig.30 Pd content of soil samples in area A-1

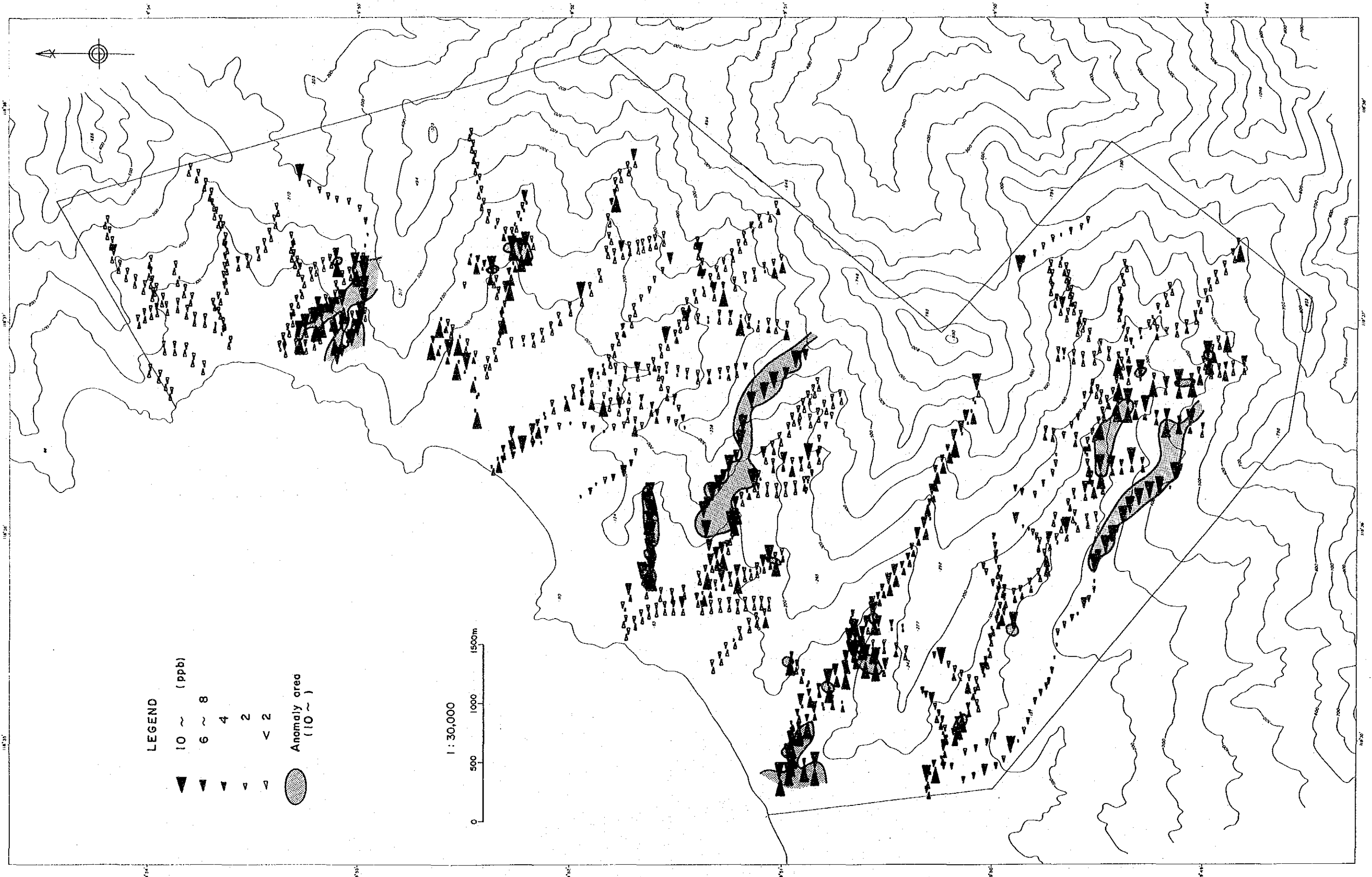


Fig. 81 Au content of soil samples in area A-1

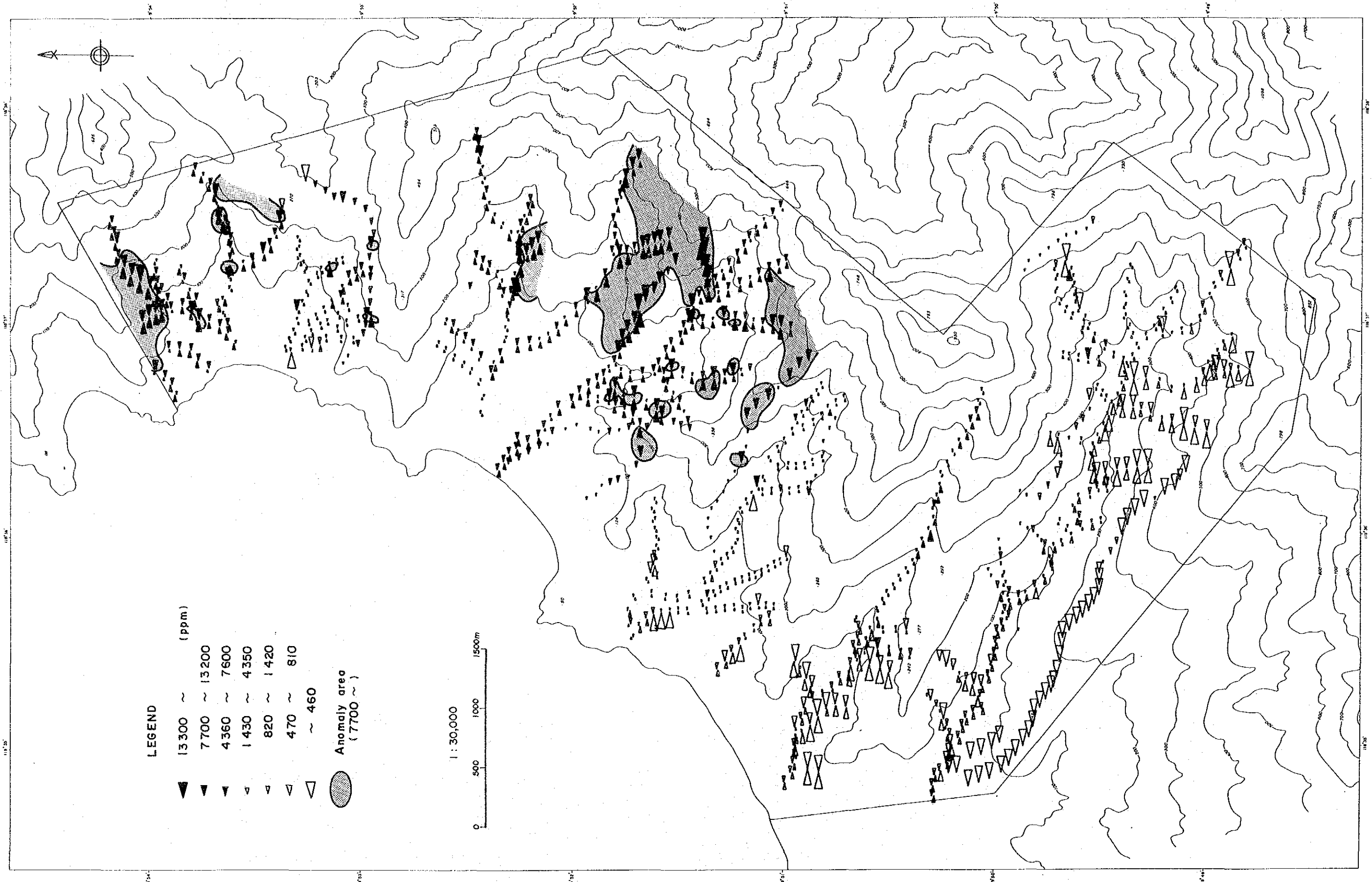


Fig. 32 Ni content of soil samples in area A-1

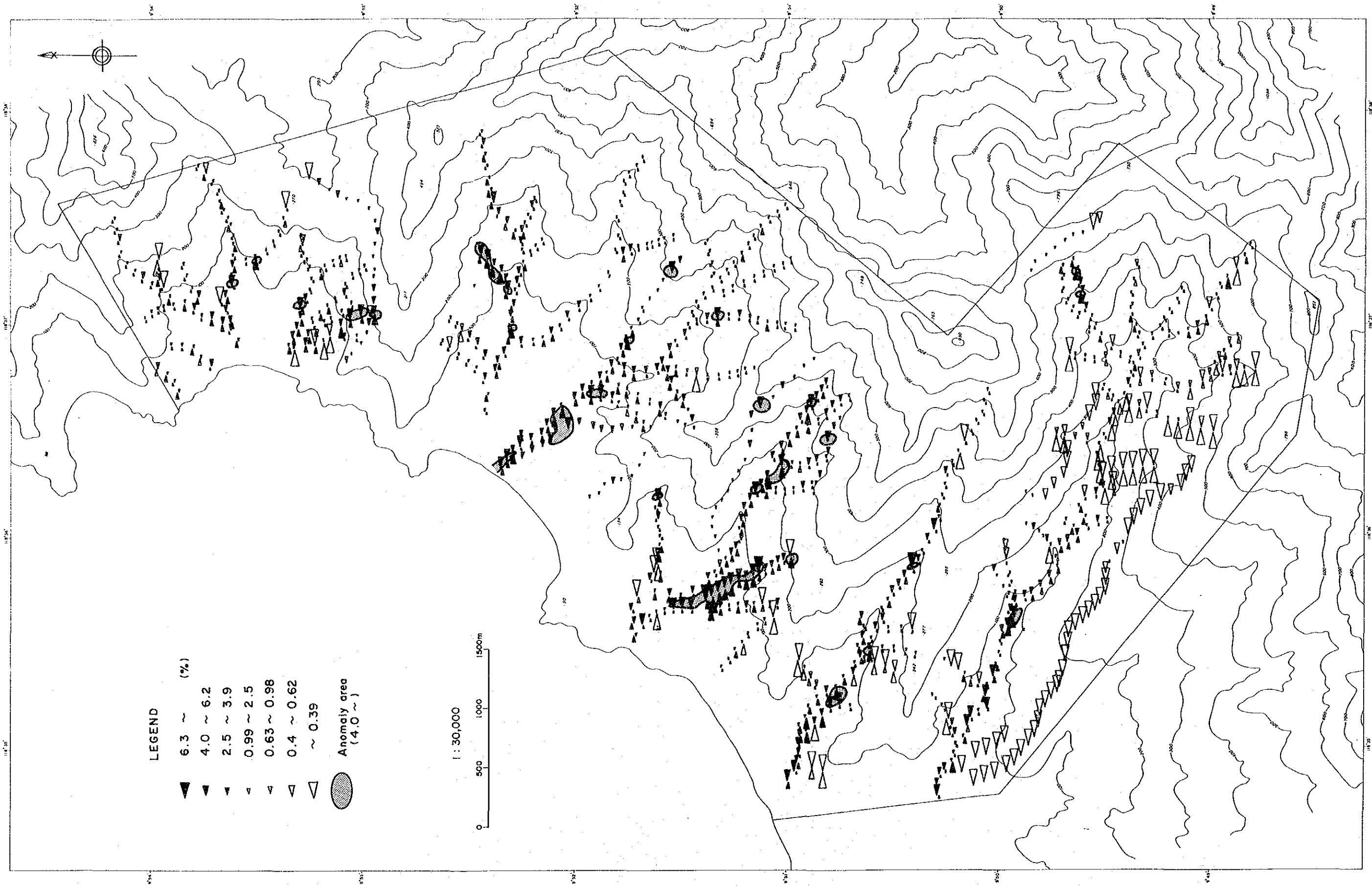


Fig.33 Cr content of soil samples in area A-1

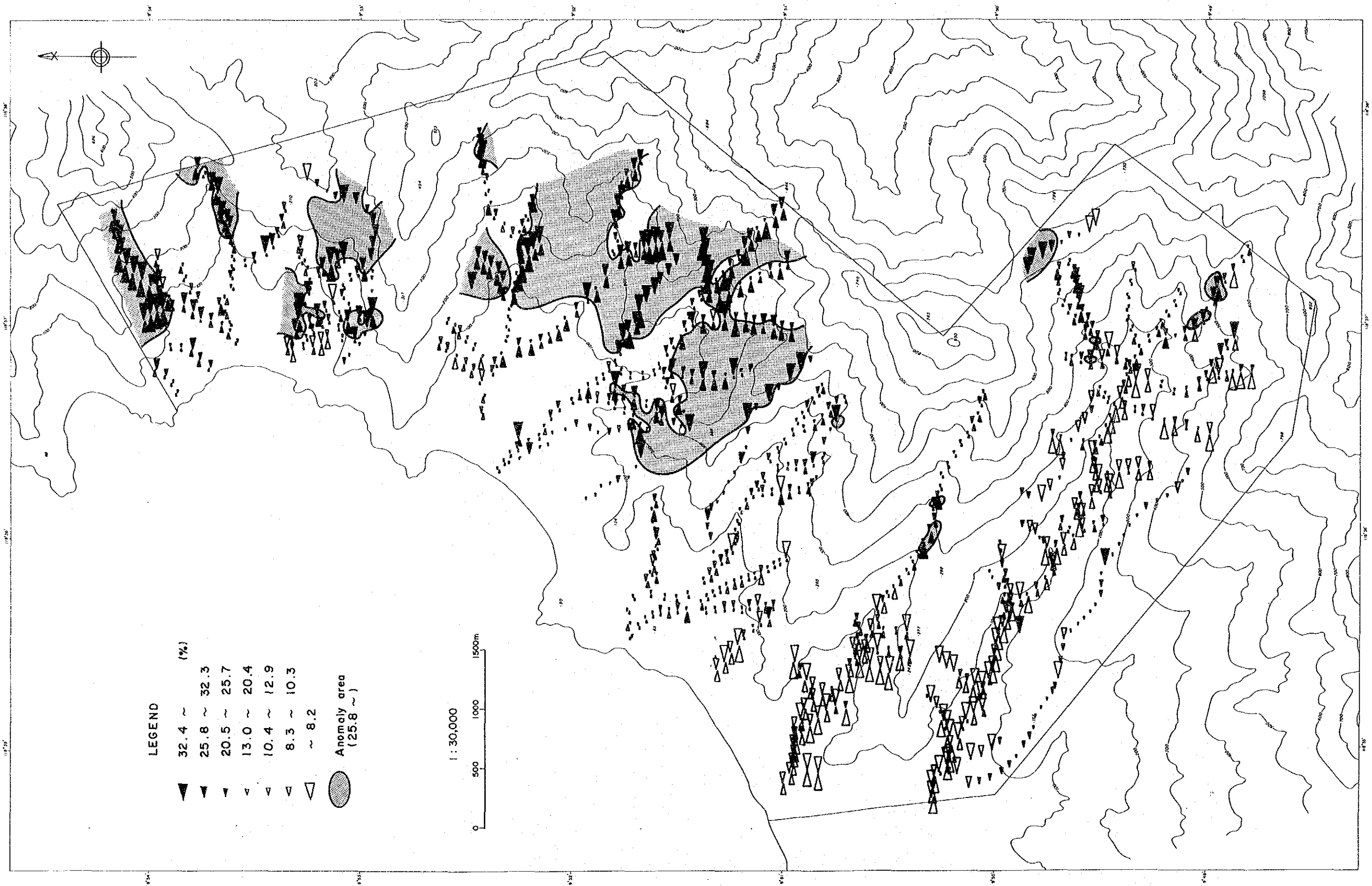


Fig. 34 Fe content of soil samples in area A-1

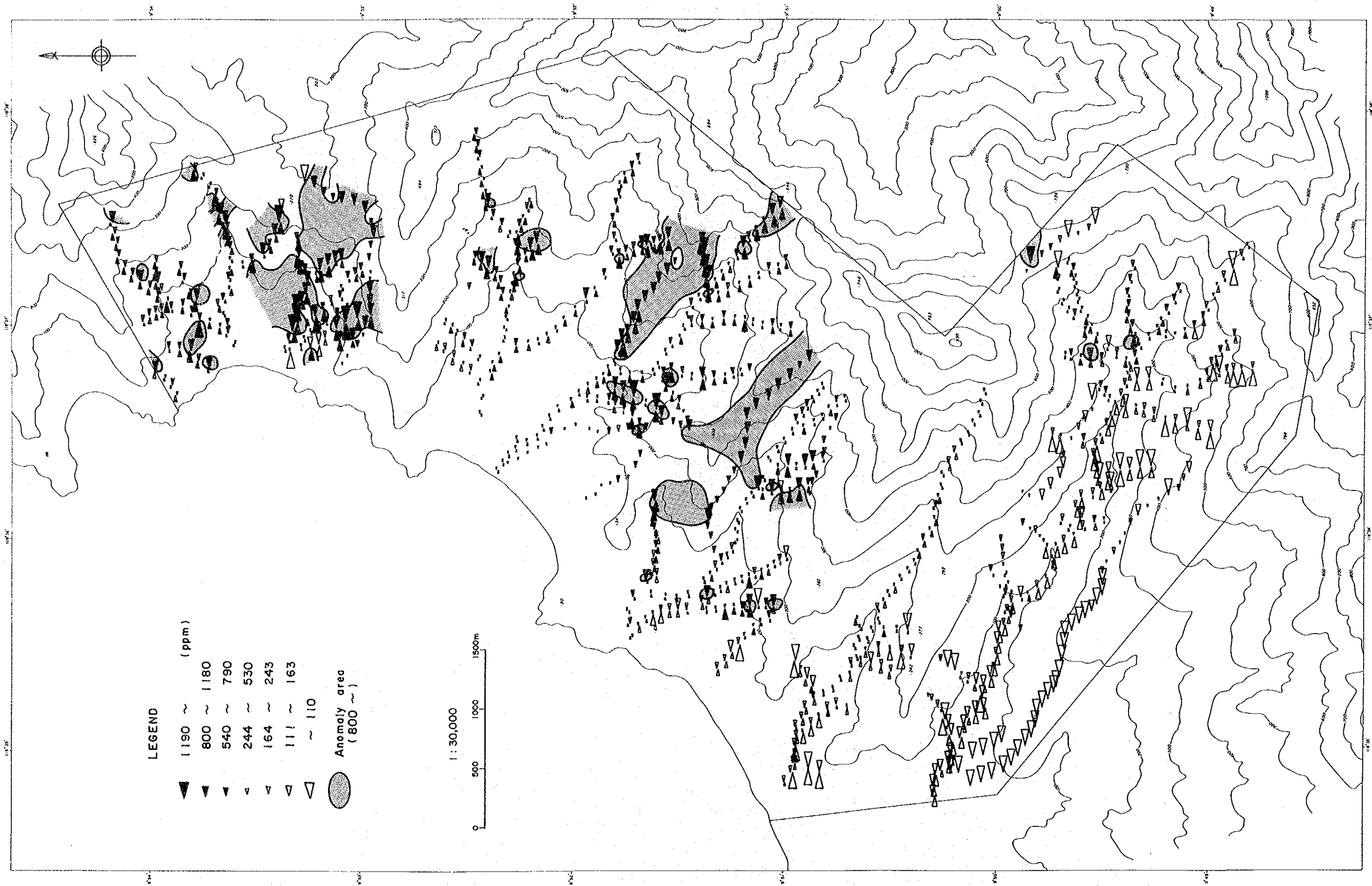


Fig.35 Co content of soil samples in area A-1

Table 9

Results of principal components analysis in area A-1

COMPONENT	EIGENVALUE	PERCENT	CUMULATIVE
Z-01	<u>3.1179</u>	44.5461	44.5461
Z-02	<u>1.8939</u>	27.0594	71.6055
Z-03	0.7350	10.5012	82.1067
Z-04	0.6663	9.5203	91.6270
Z-05	0.2813	4.0190	95.6460
Z-06	0.1917	2.7394	98.3854
Z-07	0.1130	1.6146	100.0000
TOTAL	7.0000	100	

Factor Loading

	Z-01	Z-02	Z-03	Z-04	Z-05	Z-06	Z-07
Pt	0.3787	<u>0.7668</u>	-0.3824	-0.0372	-0.3386	0.0695	-0.0334
Pd	0.0881	<u>0.9007</u>	-0.1867	0.0936	0.3533	-0.1113	0.0059
Au	-0.0989	<u>0.6692</u>	0.7294	0.0239	-0.0886	0.0379	-0.0049
Ni	<u>0.9271</u>	-0.1677	0.1166	-0.0202	-0.0243	-0.2205	-0.2217
Cr	<u>0.7651</u>	0.0118	0.0487	-0.5928	0.1460	0.1986	0.0057
Fe	<u>0.7857</u>	-0.1177	0.0241	0.5488	0.0842	0.2436	-0.0286
Co	<u>0.9459</u>	-0.0684	0.0730	0.0521	-0.0708	-0.1603	0.2487

Eigen Vector

	Z-01	Z-02	Z-03	Z-04	Z-05	Z-06	Z-07
Pt	0.2145	0.5572	-0.4460	-0.0456	-0.6384	0.1586	-0.0993
Pd	0.0499	0.6545	-0.2178	0.1146	0.6661	-0.2542	0.0175
Au	-0.0560	0.4863	0.8508	0.0293	-0.1671	0.0866	-0.0146
Ni	0.5251	-0.1218	0.1360	-0.0247	-0.0457	-0.5035	-0.6593
Cr	0.4333	0.0086	0.0568	-0.7261	0.2752	0.4535	0.0170
Fe	0.4449	-0.0855	0.0281	0.6723	0.1587	0.5563	-0.0851
Co	0.5357	-0.0497	0.0852	0.0638	-0.1336	-0.3661	0.7398

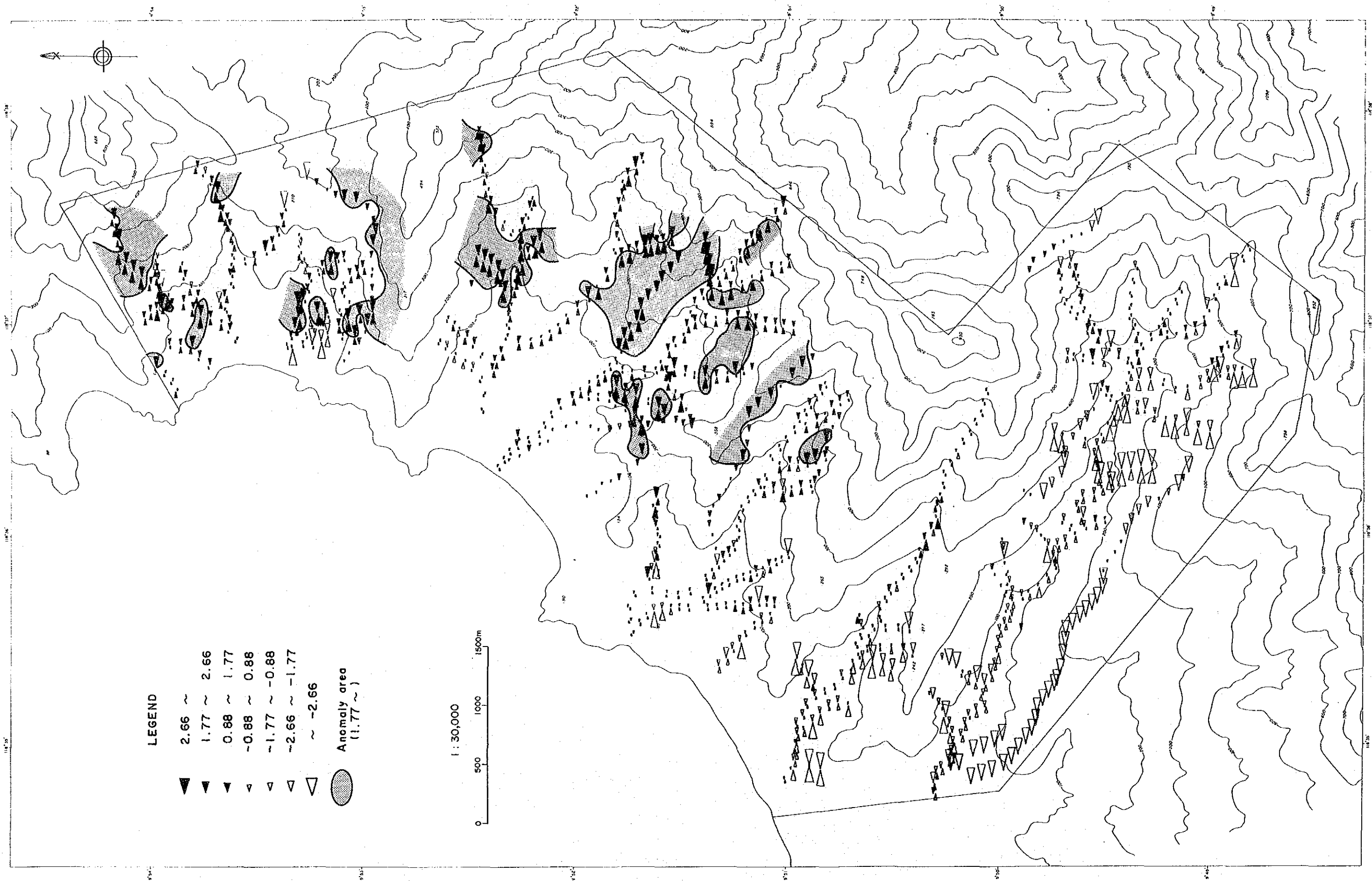


Fig. 36 Scores of principal components analysis in area A-1 (Z1)

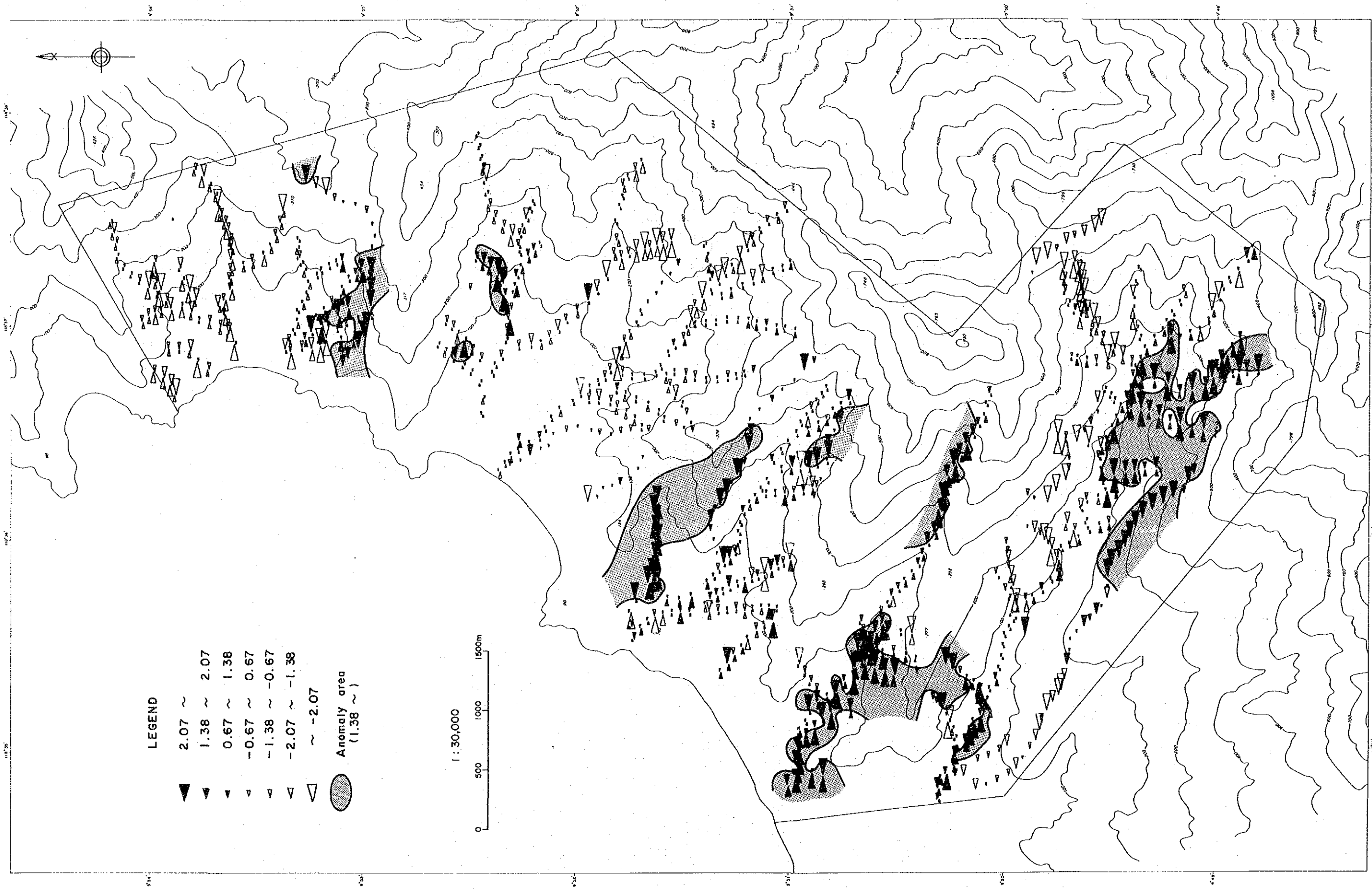


Fig. 37

Scores of principal components analysis in area A-1 (Z2)

1-6-3 Rock geochemistry

Many kinds of rocks are exposed in this area. Chemical analysis was conducted to check the differences in metal of concentration in the different kinds of rocks presenting in this area. The same elements with that of soil geochemical survey are analyzed for rock geochemistry. The number of rock samples is 123. The results of chemical analysis are shown in Appendix 13. The statistical values are shown in Table 10. These data are divided into seven groups by rock types.

A: Basalt and basaltic pyroclastics

B: Gabbroic rocks, porphyritic rocks and pegmatite

C: Harzburgite and lherzolite

D: dunite

E: Massive chromite ore

F: Pyroxenite

G: Metamorphics

Peridotite and pyroxenite have relatively high content of Pt and Pd, while others have very little Pt and Pd. The content of Au is usually very low except for some specimen from harzburgite.

Peridotites have high content of Ni and Cr, more than 1,000 ppm. Whereas other rock types contain very little Ni and Cr, less than 100 ppm. Peridotite contains twice the amount of Co compared with the other rock types.

In the peridotites, dunites have higher content of Ni and Cr than harzburgite and lherzolite. This may be due to the fact that chromite deposits of both the massive and banded types occur in the peridotite mainly within dunite bodies.

Values of Cr and Fe in peridotite are much lower than those obtained from the soil surveys but with a few exceptions. They simply suggest of the superficial concentration of chromite and iron-oxide in soils.

Table 10 Statistic quantities of rock samples in area A and A-1

	Rock type	number	range		median	linear*		logarithmic*		
						mean	std. dev.	mean	10 ⁻¹ mean	std. dev.
P t (ppb)	basalt	n=1	<5		-	-	-	-	-	-
	gabbroic	n=9	<5 - 10	<5	3.6	2.4	0.498	3.1	0.201	
	harzburgite	n=51	<5 - 80	<5	9.1	14.8	0.682	4.8	0.413	
	dunite	n=57	<5 - 75	<5	6.7	11.0	0.610	4.1	0.351	
	chromitite	n=1	<5	-	-	-	-	-	-	
	pyroxenite	n=2	<5 - 45	-	23.8	21.3	1.026	10.6	0.628	
	metamorphics	n=2	<5 - 5	-	3.8	1.3	0.548	3.5	0.151	
P d (ppb)	basalt	n=1	<2		-	-	-	-	-	
	gabbroic	n=9	<2 - 4	<2	1.3	0.9	0.067	1.2	0.189	
	harzburgite	n=51	<2 - 120	2	9.1	21.2	0.444	2.8	0.557	
	dunite	n=57	<2 - 82	<2	5.2	11.7	0.351	2.2	0.473	
	chromitite	n=1	<2	-	-	-	-	-	-	
	pyroxenite	n=2	2 - 36	-	19.0	17.0	0.929	8.5	0.628	
	metamorphics	n=2	<2 - 2	-	1.5	0.5	0.151	1.4	0.151	
A u (ppb)	basalt	n=1	<2		-	-	-	-	-	
	gabbroic	n=9	<2 - 4	<2	1.4	1.0	0.100	1.3	0.201	
	harzburgite	n=51	<2 - 42	<2	2.3	6.0	0.100	1.3	0.307	
	dunite	n=57	<2 - 6	<2	1.3	1.1	0.059	1.1	0.183	
	chromitite	n=1	<2	-	-	-	-	-	-	
	pyroxenite	n=2	<2 - <2	-	1.0	0.0	0.000	1.0	0.000	
	metamorphics	n=2	<2 - <2	-	1.0	0.0	0.000	1.0	0.000	
N i (ppm)	basalt	n=1	70		-	-	-	-	-	
	gabbroic	n=9	3 - 2620	60	316.2	814.9	1.412	25.8	0.871	
	harzburgite	n=51	40 - 2910	2240	1852.5	820.5	3.139	1377.3	0.461	
	dunite	n=57	820 - 3430	2470	2241.9	664.6	3.328	2129.8	0.146	
	chromitite	n=1	500	-	-	-	-	-	-	
	pyroxenite	n=2	160 - 1750	-	955.0	795.0	2.724	529.2	0.519	
	metamorphics	n=2	50 - 130	-	90.0	40.0	1.906	80.6	0.207	
C r (ppm)	basalt	n=1	<100		-	-	-	-	-	
	gabbroic	n=9	<100 - 1700	<100	255.6	512.3	1.975	94.4	0.485	
	harzburgite	n=51	<100 - 17000	1700	2168.4	2827.3	3.159	1443.5	0.404	
	dunite	n=57	500 - 54000	2400	4978.9	9008.9	3.444	2778.6	0.383	
	chromitite	n=1	148000	-	-	-	-	-	-	
	pyroxenite	n=2	<100 - 2000	-	1025.0	975.0	2.500	316.2	0.801	
	metamorphics	n=2	<100 - 200	-	125.0	75.0	2.000	100.0	0.301	
F e (%)	basalt	n=1	5.7		-	-	-	-	-	
	gabbroic	n=9	0.3 - 4.2	2.3	1.7	1.5	0.014	1.0	0.461	
	harzburgite	n=51	1.2 - 7.0	4.3	4.1	1.0	0.591	3.9	0.144	
	dunite	n=57	1.8 - 8.2	4.5	4.8	1.1	0.669	4.7	0.102	
	chromitite	n=1	0.5	-	-	-	-	-	-	
	pyroxenite	n=2	1.4 - 4.3	-	2.9	1.5	0.390	2.5	0.244	
	metamorphics	n=2	0.8 - 3.2	-	2.0	1.2	0.190	1.5	0.315	
C o (ppm)	basalt	n=1	48		-	-	-	-	-	
	gabbroic	n=9	14 - 63	55	44.2	17.0	1.602	39.9	0.213	
	harzburgite	n=51	29 - 281	93	91.8	35.2	1.936	86.3	0.154	
	dunite	n=57	39 - 137	91	90.4	21.4	1.943	87.7	0.109	
	chromitite	n=1	125	-	-	-	-	-	-	
	pyroxenite	n=2	46 - 97	-	71.5	25.5	1.825	66.8	0.162	
	metamorphics	n=2	2 - 380	-	191.0	189.0	1.440	27.6	1.139	

*:Half of the detection limit value is used for the below-detection-limit data.

1-7 Discussion

The project area is underlain by the Palawan Ophiolite, the Kabangan Metamorphics (UNDP,1985), the Tagbuos Siltstone, and the Sulu Sea Mine Formation. The Palawan Ophiolite is distributed in a large area, and consists of the Mt. Beaufort Ultramafics, the San Vicente Gabbro, the Stavely Range Gabbro, and the Maranat Pillow Basalt (UNDP,1985) from the bottom. Each formation has been sheared by thrust faults during the ophiolite thrust movement, and imbricated as presently seen. In the field the uppermost lithology, which is the Mt. Beaufort Ultramafics, overlies other formations as a nappe. The Bacungan Window and the Iratag Window have been formed by the erosion of the Mt. Beaufort Ultramafics.

The most important mineral occurrences in the area are the chrome and the nickel, which are hosted by the Mt. Beaufort Ultramafics. The observed outcrops of chromitites are small in scale, only several meters wide, consisting of lenses, pods, or disseminated seams. Most of these were found as the results of the detailed geological and geochemical surveys in area A-1, which was selected based on the results of the initial geochemical survey in the A-area. Most of the chromite showings are in dunite tectonite, which intruded as diapir-like bodies into harzburgite. Some occurrences are in harzburgite too, however these are of small scale and quite few. It is possible to say that the distribution of dunite bodies controls the location of chromite occurrences.

Nickel laterite has been formed by weathering of peridotites in this area. Laterite occurrences, in which iron hydroxide have concentrated on the surface, are distributed in the Bacungan area in the northern part and the basin of the Tagkawayan River in the west coast. The depth of the lateritic layers in the Bacungan area is very deep, therefore most of the test pits digged in the area up to a depth of 5 meters did not reach altered peridotite zones, in which nickel is concentrated. Some test pits in the western part have revealed nickel occurrences, but the area is poor in laterite due to steep topography. The important factors for forming nickel-laterite zones are the topography and the level of groundwater, which give strong influences to weathering processes, than nickel contents of host rocks.

In the geochemical survey in the A-area, volume ratios of heavy minerals were investigated by panning in sites as well as soil sampling. This method is effective in case enough water is available in sites, and to delineate promising areas promptly for further works at the early stage of the survey. The seven elements assayed in the soil geochemistry can be classified into two categories based on their behavior. One is a group of Ni, Cr, Fe, and Co, relating to chromium, and the other is a group of Pt, Pd, and Au relating to precious metals. Interpretation of the geochemical anomalies of the both groups lead the extraction of three potential areas; the area north of Tagburos, the area from north of Bacungan to the west coast, and the area from the Malinao River to Tagminatay in the west coast.

The results of the soil geochemical survey in the A-area lead the selection of detailed survey area A-1, the area from the Malinao River to Tagminatay. As a result of the geochemical survey done in area A-1, the two groups of assayed elements, relating to chromium and precious metals respectively, show geochemically different behavior. However the following two areas show some overlap of anomalies of these two groups, and are judged as promising areas for further exploration activities; i.e. the area containing the Pananlagan mineral showings and the area from the Tagkawayan mineral showings to Tagminatay.

This year's survey has revealed that the in-situ soil geochemical survey was effective to delineate chromite deposits' areas. However, some mineral showings did not show any geochemical anomalies in spite of its formation under the same environment, like the case of the Macasaet occurrences. This case probably shows that in some cases chromium contents are rather less in areas around ore deposits due to strong mineral concentration into ore bodies from high chromium content host rock areas.

Chapter 2 B-area and Detailed Survey area B-1

2-1 Location and transportation

The B-area is situated the south central part of Palawan Island to the southeast of Puerto Princesa, the capital city of the Province of Palawan. It is extended from the east coast to the west coast, and between 9°07'N and 9°40'N in latitude. The area is falls under two jurisdiction; its eastern half under Narra province and its western half under Quezon province.

The subcamp in Narra, which was set up for the survey in the southwestern B-area, is accessible from Puerto Princesa by highway, and it takes two hours by car. This highway leads to Rio Tuba, the southern end of this island. A branch of this road from Aboabo leads to Quezon, located on the west coast. From Quezon to the southwestern B-area, the road is not completed in some parts.

On the other, no vehicle roads run in the west coast. So we arrived the western part of survey area by small boat (bancha) from Quezon and from coast on foot.

The detailed survey area B-1 is located in the southeastern B-area. It is 10km northwest of Narra, and on the southwest of the Norsophil Mine (ex-Trident Mine). It is accessible by car from Narra to the survey area, but no vehicle road exists within the area.

2-2 Topography and drainage

The great part, especially the ultramafic rocks distribution area, forms rugged mountains in this survey area. In where, deep valleys have been dissected, and waterfalls exist in many places.

The Victoria Range stretches from NE to SW in the B-area. This range has many high mountains more than 1,000 meters above sea level, in which the highest point is Victoria Peak (1,978m), and separates east and west watersheds. On its' eastern side, there is a narrow plain along the east coast. While on its' western side, the flatland is only the vicinity of large rivers' mouths.

The detailed survey area B-1 is in a mountainous area. The Panacan River runs on the

northeastern side, and the Malinao River runs on the southwestern side. Both rivers run down to the southeast into the Sulu Sea.

2-3 Climate and vegetation

It is said that the season of Palawan Island is distinctly divided into rainy season and dry season. There is some different climate between west coast and east coast.

In the west coast rainy season is from June to November and dry season is from December to May. While east coast can not distinguish clearly.

2-4 Survey method

1) Geological Survey

(1) B-area

The survey in the B-area was done using topographic maps on the scale of 1:10,000, which were enlarged from its original 1:50,000. Survey routes were set up along streams. The route length is 400km in total. The results were recorded on the 1:10,000 scale route maps. Samples were taken for laboratory studies and geochemical investigations. A subcamp was set up at Narra for the survey for the east coast area. For the survey, also a mobile camp was used. The survey for the west coast area was performed from the camp set up at Quezon. A banca boat and mobile camp were also used for the survey.

(2) Detailed Survey area B-1a/B-1b

Geological survey for area B-1a was conducted using maps on the scale of 1:10,000, which were enlarged from its original 1:50,000. Survey routes were set up for main stream lines and partially on ridges. A simple topographic survey using a compass and tape was also conducted. The route length is 40km in total. Results were recorded on route maps on a scale of 1:10,000.

The geological survey in area B-1b was conducted on the scale of 1:5,000. The length of this survey route is 50km in total. The results were recorded on the base maps on a scale of 1:5,000. In both detailed survey areas, samples were taken for laboratory studies and geochemical

investigations.

The surveys in the areas were also conducted from the subcamp set up at Narra, and using a mobile camp.

2) Pit Surveys

Test pit surveys were conducted in the eastern part of B-1a and central south part of B-1b to clarify dunite distribution areas and to find chromite ores. Total 30 pits were dug in the two zones, 15 each for two.

The pits are 1m x 1m in size and 1.2m to 3m deep. They were dug by hands using shovels, iron staffs, ropes and pulleys.

Soil profiles of the pits were sketched on the scale of 1:50. Samples were taken from each soil horizon or every one meter.

2-5 Geology

2-5-1 Outline of geology

The B-area is underlain by the Panas Formation of Eocene age, the Palawan Ophiolite which is thrust over the Panas Formation during late Eocene time, and unconformably overlying the Ransang Formation, the Isugod Formation, the Alfonso XIII Formation, and the Iwahig Formation of Miocene to Pliocene age, and alluvium.

The Panas Formation consists of siliceous shale, phyllitic shale, siliceous sandstone, and chert. It is distributed in the surrounding area of Berong and south of Moorsom Point in the west coast, and the upstream areas of the Malasgao River and Panacan River as windows in small scale.

The Palawan Ophiolite is dominant in the B-area, and is composed of harzburgite and dunite of the Mt. Beaufort Ultramafics, layered gabbro of the Sultan Peak Gabbro, and diabase and basalt of the Espina Basalt.

The Inagauan Metamorphics, consisting of quartz-mica schist, green schist, and amphibolite.

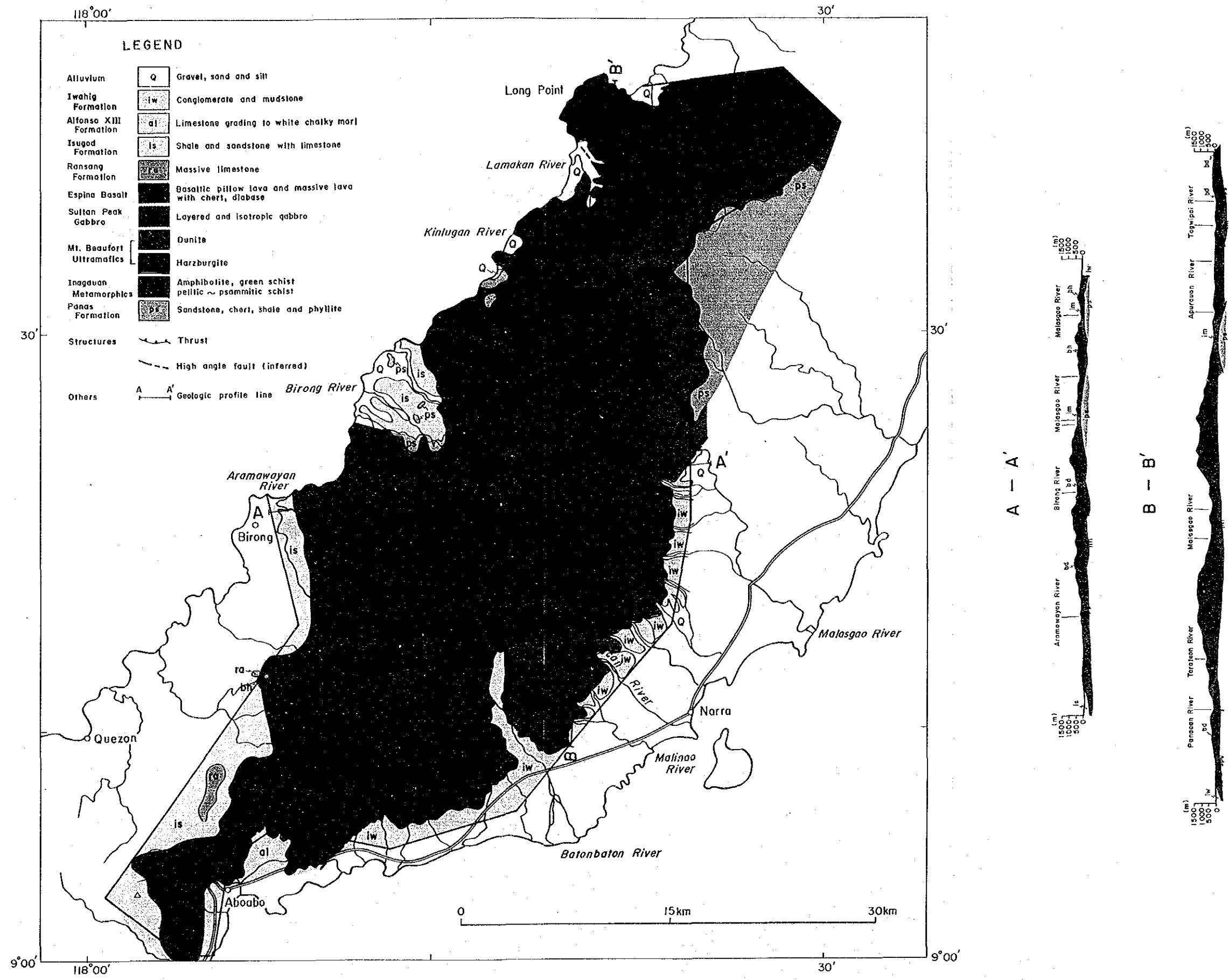


Fig. 38 Geologic map and profile in area B

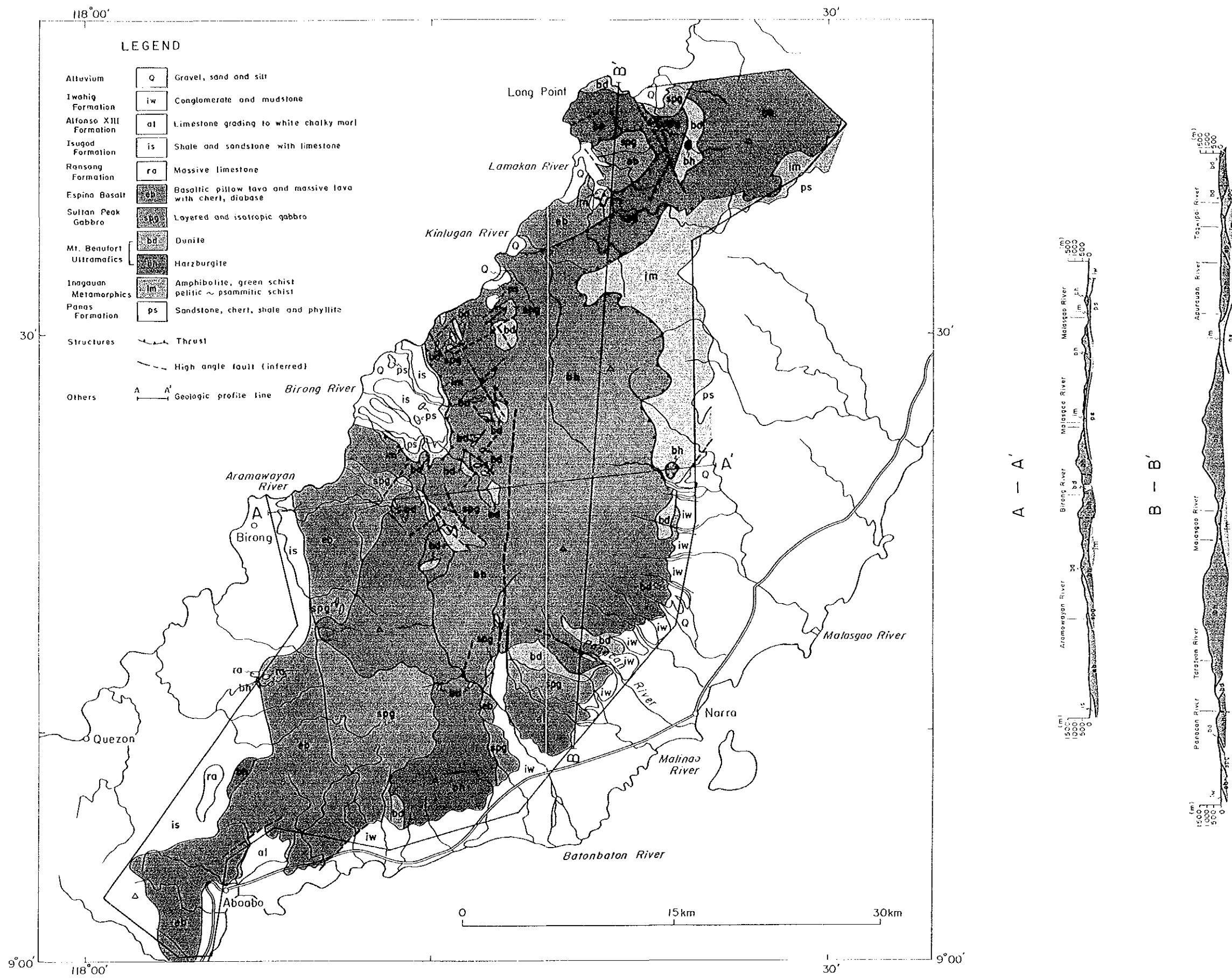


Fig. 38 Geologic map and profile in area B



Fig. 38 Geologic map and profile in area F

Age	Geologic Column	Rock Description	Formation/Rock Unit	Mineral Showings
Quaternary	Q	Gravel, sand and silt ~unconformity~	Alluvium	● Secondary deposits in Berong area
Pliocene	iw ?	Conglomerate, mudstone ?	Iwahig Formation	
Late	al	Coral and reef limestone ~unconformity~	Alfonso XIII Formation	
Miocene Middle	is	Shale, sandstone with limestone ~unconformity~	Isugod Formation	
Early	ra	Massive limestone ~unconformity~	Ransang Formation	
Late Cretaceous	v v v v v v v v v v v v	Basaltic pillow lava, massive lava, chert	Espina Basalt	Crustal Sequence
	v v v v v v v v v v v v	Diabase		
	> > > > > > > > > > >	Isotropic gabbro, layered gabbro		
	spg	Cumulate dunite troctolite		
Eocene	bd	dunite tectonite (dikes) fine grained gabbro pegmatitic gabbro pyroxenite	Mt. Beaufort Ultramafics	● Cr dissemination in B-1 area Mantle Sequence
	bh bd bd di	Harzburgite thrust		● Norsophii Cr mine ● Cr ore deposits in Long Point
	im	Amphibolite, Greenschist thrust	Inagauan Metamorphics	Metamorphic Sheets
	ps	Quartz mica schist, quartz schist grade	Panas Formation	
		Sandstone, chert, shale phyllite		

Fig. 39 Schematic geologic map in area B

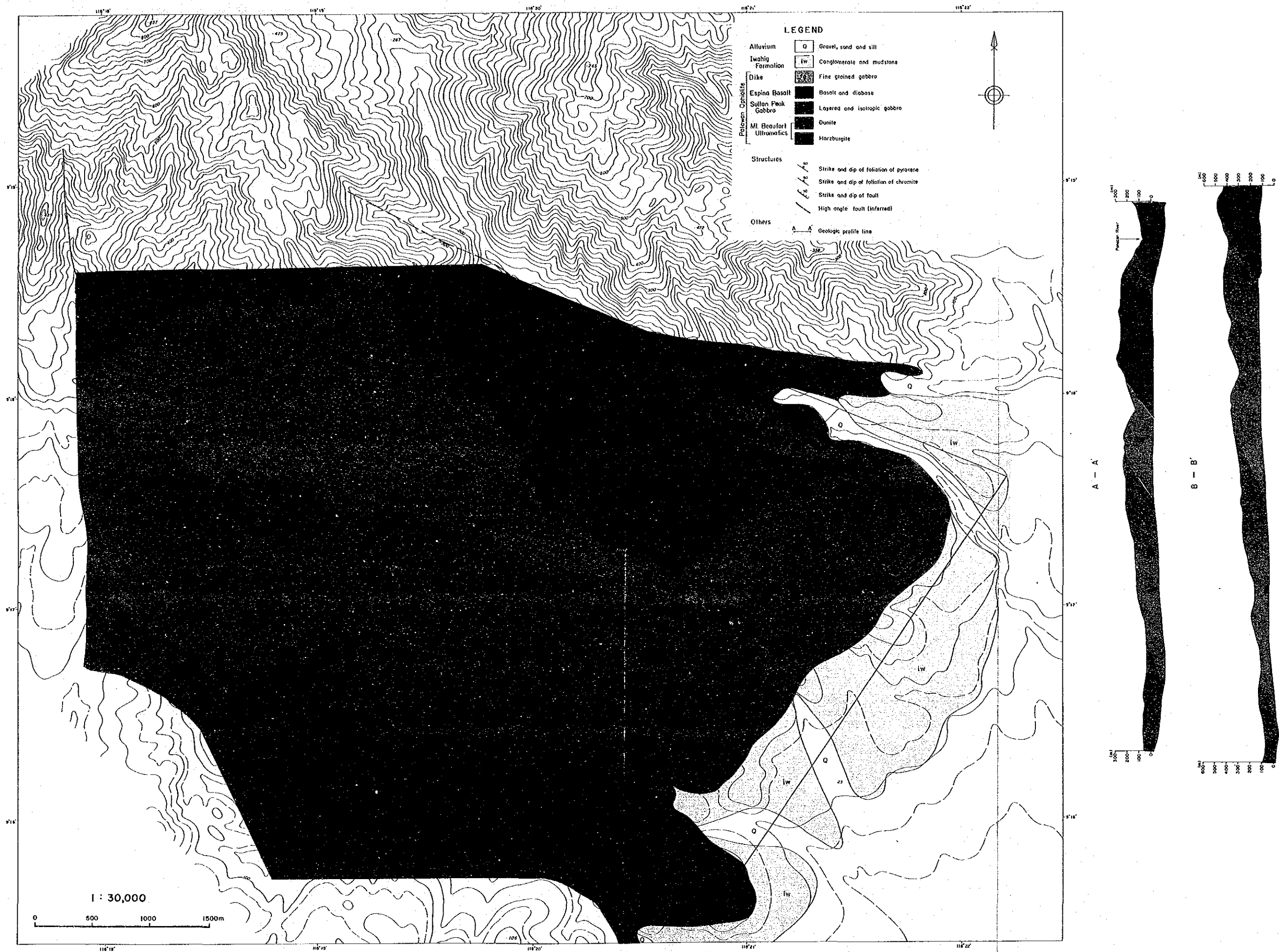


Fig. 40 Geologic map and profile in area B-1a

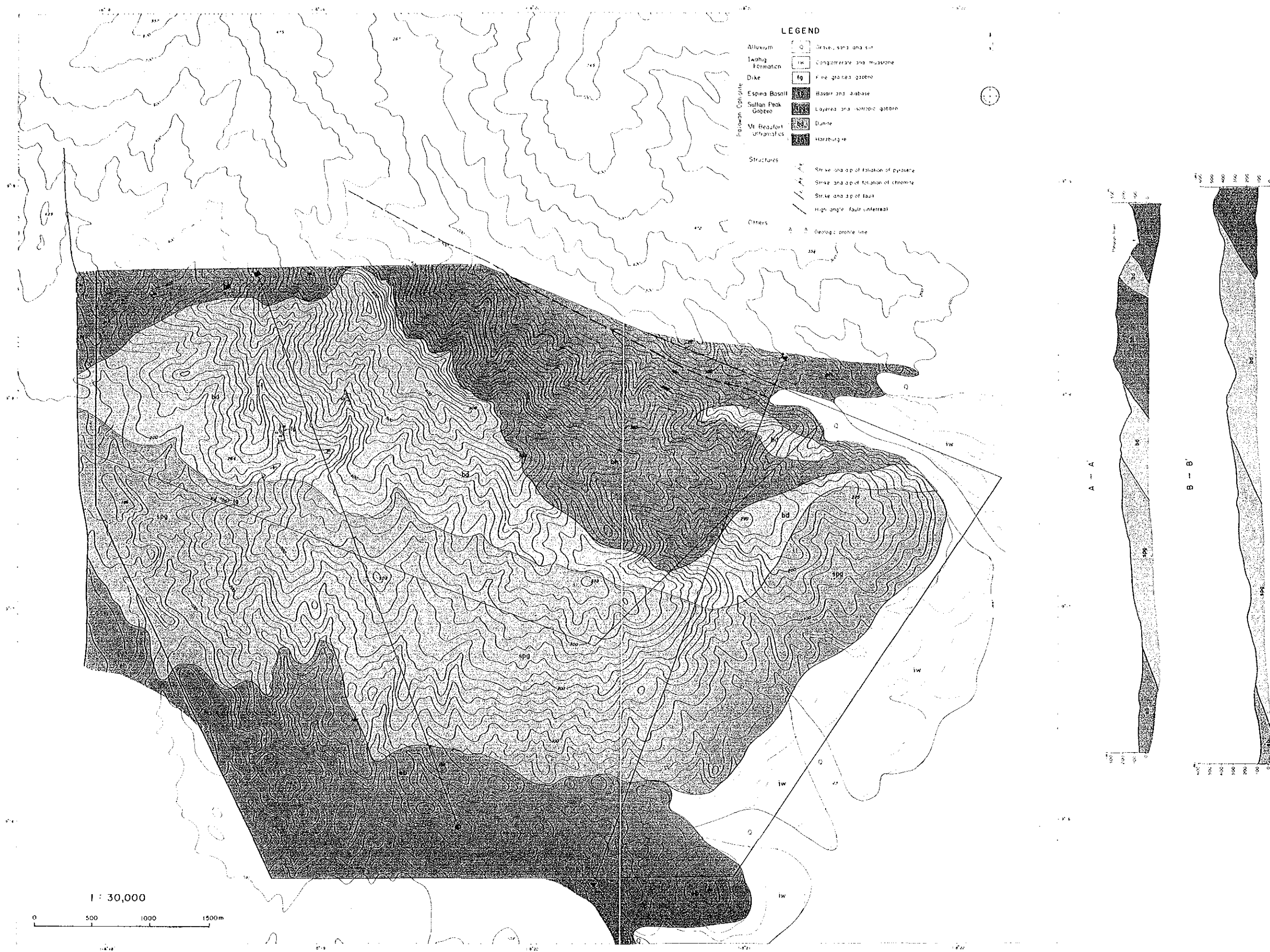


Fig. 40 Geologic map and profile in area B-1a

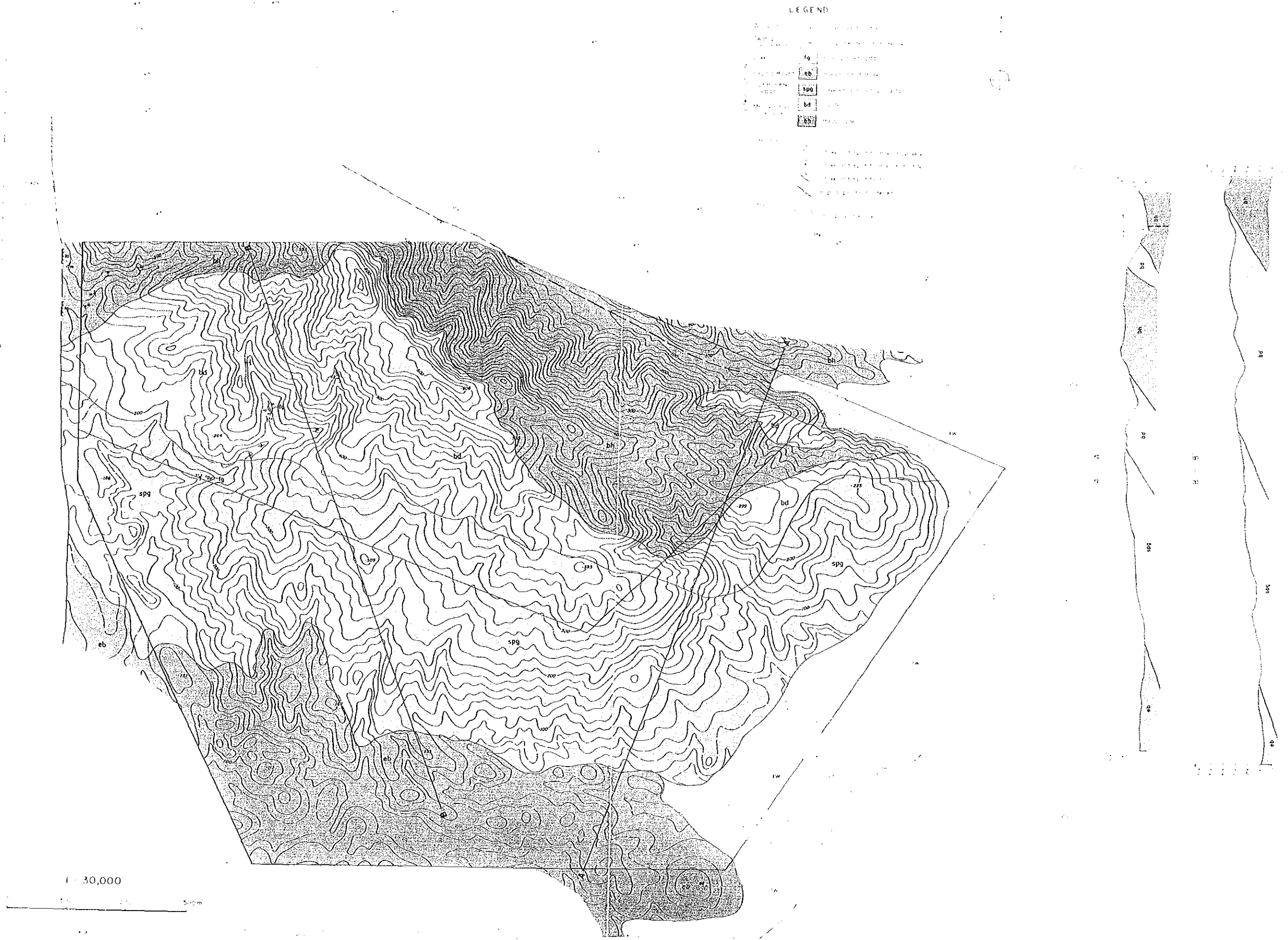


Fig. 10 Geologic map and profile in area B 1a



Fig.41 Geologic map in area B-1b

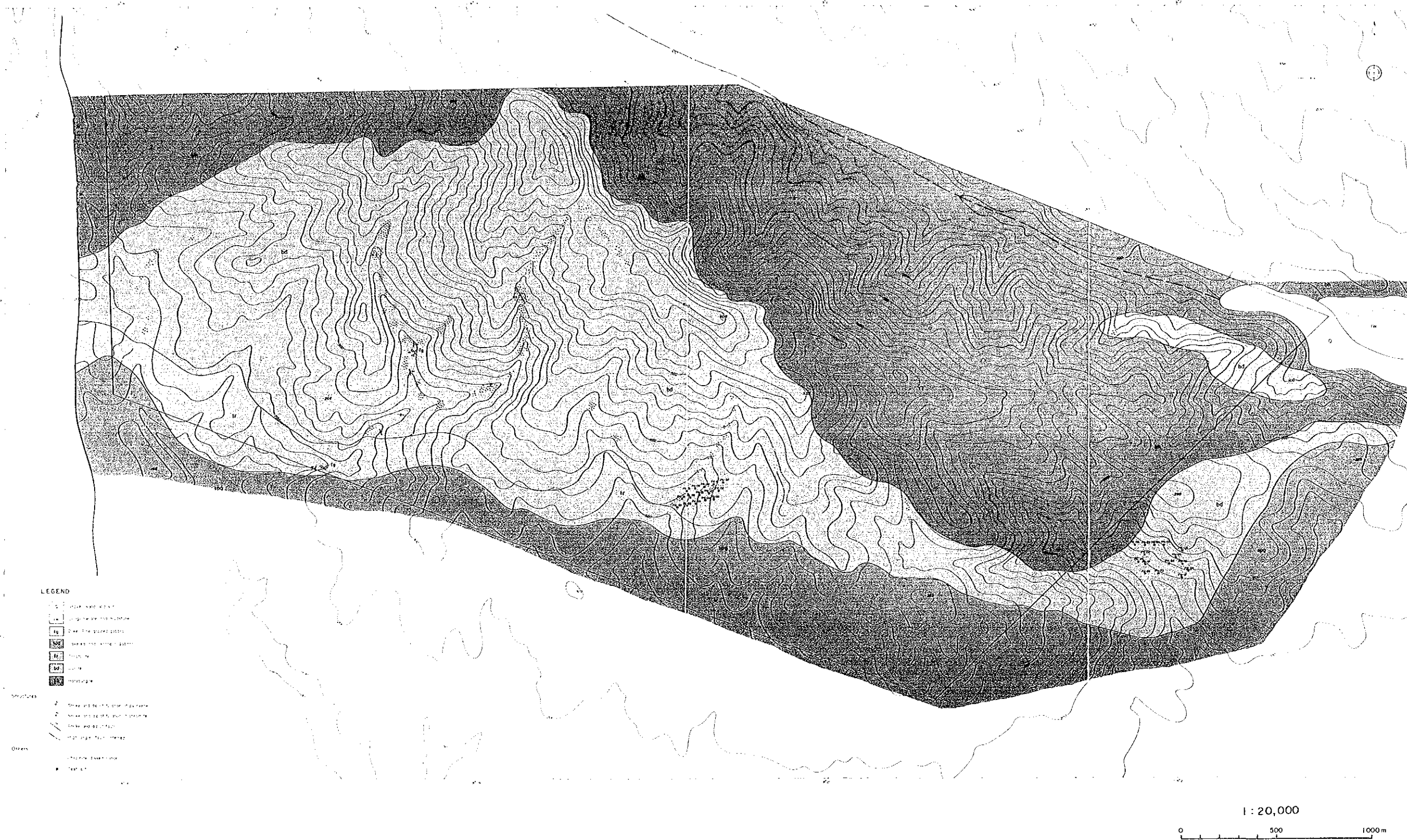
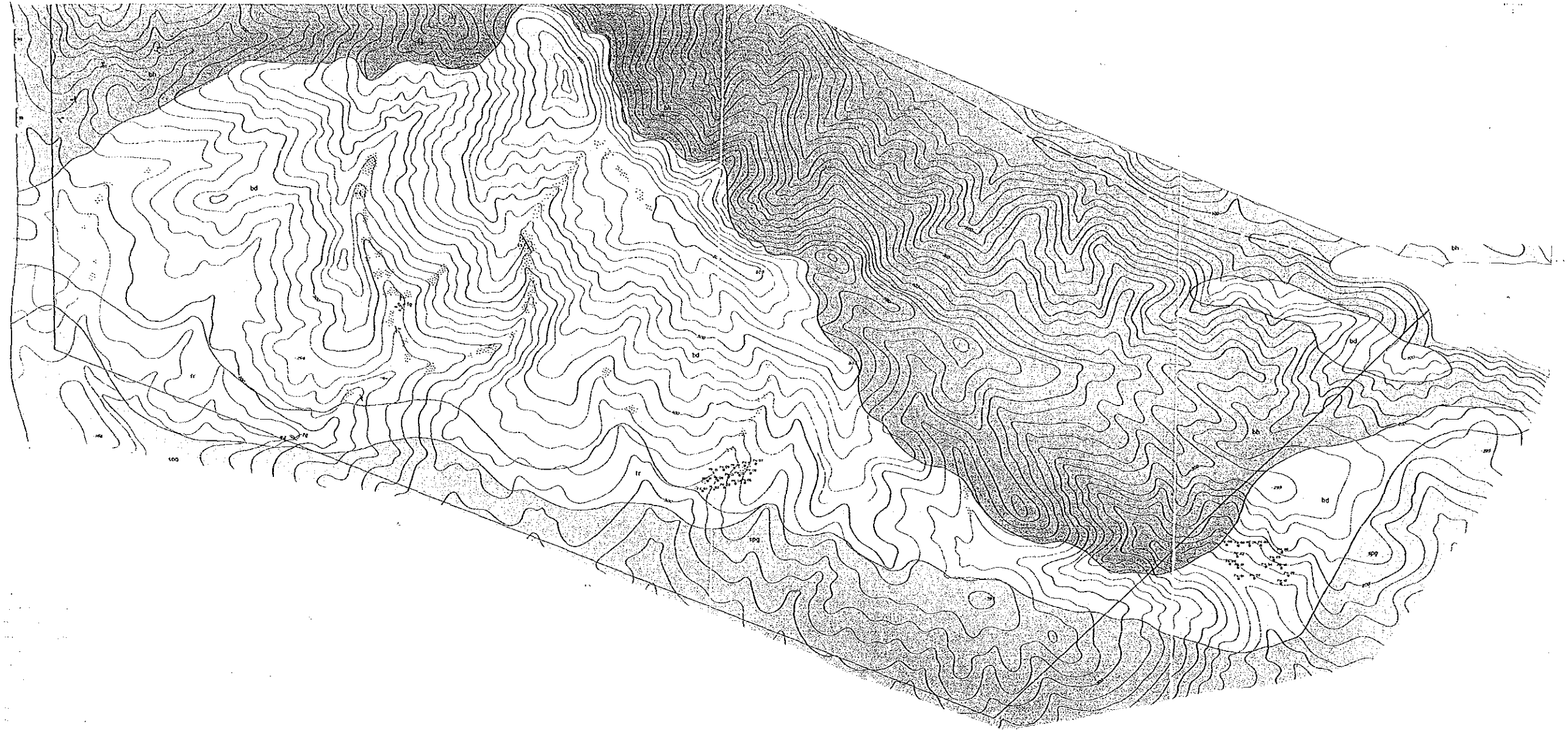


Fig.41 Geologic map in area B-1b



1 : 20,000

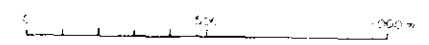


Fig. 11 Geologic map in area B 1b

They are believed to have formed due to dynamic metamorphism along the thrust fault during the thrusting and emplacement of the ophiolite sheet.

The Ransang Formation and later formations are distributed in the lowland areas of the east and west coasts, overlying the Palawan Ophiolite.

The thrust fault between the Panas Formation and Palawan Ophiolite are almost horizontal in the angle. A left lateral, high angle fault exists in the central B-area, which trends south to west. The geological structure is different in the eastern side and western side of this fault. The ophiolite in the eastern side trends WNW to ESE and dips SSW, while the ophiolite in the western side trends NNW to SSE and dips SW.

The detailed survey area B-1 is underlain by the Mt. Beaufort Ultramafics, the Sultan Peak Gabbro, and the Espina Basalt. The Iwahig Formation is distributed in the lowland areas of the eastern area, overlying these rocks.

2-5-2 Detailed geology

1) Panas Formation

The Panas Formation is distributed in the upper part of the Inagauan River --in the northeastern B-area, the area around Berong River and the vicinity of Tagbolante River --in the west coast. This Formation consists of siliceous shale, phyllitic shale, siliceous sandstone, and chert. The siliceous shale and chert are pink, red, brown, and dark gray, and have distinct stratification. The phyllite is greenish gray, and accompanied by quartz veinlets. The sandstone is grayish green, and hard, compact, fine grained equi-granular rock. It have been slightly metamorphosed. The metamorphic grade tends to increase near the Inagauan Metamorphics.

This Formation strikes N-S to N30°E, and dips 50° to 80°NE. Judging from the nannofossil and foraminifera yielded here, it is reported as of Eocene age.

2) Inagauan Metamorphics

The Inagauan Metamorphics is distributed in the northeastern B-area and the area underlain

by the Panas Formation around Berong on the west coast. They overlie on the Panas Formation, and consist of quartz-mica schist, quartz schist, green schist, and amphibolite.

The quartz-mica schist and quartz schist are distributed in three areas: 1) the upstream area of the Inagauan River, 2) the mid and upstream area of the Malasgao River in the northeastern B-area, 3) in the hills around Berong on the west coast. They are pale gray to pale pink, and mainly consist of quartz and plagioclase, which are 0.1mm to 0.5mm in size, being accompanied by muscovite. They have intense schistosity and microfoldings, and trend N-S, dip 60°SE near Berong on the west coast. Those in the northeastern area of the Malasgao River has a schistosity trending N-S, dipping 25°NW. The results of the K-Ar dating of the quartz-mica schist indicates 45.6 ± 6.8 Ma (JICA and MMAJ, 1989).

Green schist and amphibolite are distributed in the following areas; the uppermost-stream area of the Inagauan River and the upstream area of the Malasgao River in the northeastern B-area, and the border zone between the hills and mountains around Berong in the west coast. The green schist is pale blue to bluish gray, and having been undergone intense shearing. Amphibolite is bluish gray. They show banded structure consisting of amphibole rich parts and feldspar rich parts. Quartz veinlets, in some places, are observed along the schistosity of the green schist and amphibolite.

Around Berong, these rocks commonly show schistosity of NE-NNE to SW-SSW dipping 30° to 80°SE, in some cases 50°NW. It is presumed that there exists microfoldings with a axis trending NE-NNE to SW-SSW. In the area along the Malasgao River, microfoldings trend NNW to SSE and dip 60°NW. The result of the K-Ar dating of the amphibole from the upstream area of the Malasgao River indicates 37.2 ± 1.9 Ma (JICA and MMAJ, 1987).

3) Mt. Beaufort Ultramafics

The Mt. Beaufort Ultramafics are dominantly distributed in the central to northern B-area, and consist mainly of harzburgite accompanied by dunite in some places.

Fresh harzburgite is greenish gray, but weathered parts are pale brown. It consists mainly of olivine, several millimeters in size, accompanied with orthopyroxene. Both minerals have

undergone serpentinization. The harzburgite commonly hosts for chromite.

Dunite consists of olivine, 4mm to 5mm large, and have undergone serpentinization in part or in the most of part. It can be divided into two kinds; 1) dunite of the cumulate member, being directly overlain by the gabbro, 2) dunite tectonite, which intruded into the harzburgite as diapir-like bodies.

The cumulate dunite is greenish gray in fresh parts, while pale brown in weathered parts. The transitional zones with overlying gabbro and troctolite exist in some places, which show banded structure of both rock units. The dunite has undergone serpentinization, and is accompanied with a small amount of chromite.

The dunite tectonite is also accompanied with chromite. The direction of chromite seams and lenses seems to be arranged in the same direction of a dunite tectonite bodies's trend. in a layer or lens. The chromium deposit in the Norsophil Mine is contained in the diapir-like bodies of dunite tectonite.

The cumulate dunite is distributed in the area northwest of Narra in the central part of the east coast, and the area southeast of Berong in the central part of the west coast.

The cumulate dunite in the northwest of Narra trends WNW to ESE, approximately 6km long and 100m to 200m thick, and dips 20° to 30°SW. The cumulate dunite in the southeast of Berong trends NW-NNW to SE-SSE, approximately 200m to 300m thick, and dips 20° to 30°SW.

The dunite tectonites are commonly small scale with 1m to 2m in width. Some dunite bodies are rather large, one of the largest dunite tectonite body one which contains the Norsophil Deposit trends WNW to ESE, approximately 4km long, 1km wide. Judging from the shape of the other small scale diapir-like dunite bodies, it probably dips at a deep angle towards the northeast. The diapir-like dunite bodies commonly appears to cut the foliation of the harzburgite.

The foliation of harzburgite formed by the orthopyroxene are observed. Its orientation differs in parts of the B-area. It trends NNW to SSE and E to W dipping to the south in the basin of the Tagbolante River in the central area of the east coast and on the west coast. In the northern west coast, it trends NEN to SWS and dips south in some cases. In the east coast side, it trends commonly NE to SW and NW to SE, and dips north, but in some cases dips south.

Judging from the structure and its distribution area of the cumulate dunite, it is assumed that the Mt. Beaufort Ultramafics generally trend NW to SE, and dip gently to the southwest. Accordingly, the southwestern side is of upper, and the northeastern side is of lower.

The Mt. Beaufort Ultramafics is thrust over the Panas Formation. In between these two, the Inagauan Metamorphics exist as metamorphic sheets. On the upper part of the Malasgao River, the Mt. Beaufort Ultramafics near the metamorphic rocks have undergone shearing and mylonitization.

4) Sultan Peak Gabbro

The Sultan Peak Gabbro is distributed in the area centered by Sultan Peak situated in the southern B-area as a large scale intrusive mass, covering the eastern and western sides of the backbone mountains. It is also distributed to the west of Narra in the east coast, to the south of Berong and around Long Point in the west coast.

The rocks are pale greenish gray, medium grained gabbro to olivine gabbro, and mainly consist of plagioclase and clinopyroxene, accompanied with olivine in some cases. The plagioclase is usually fresh, but sometimes has altered to prehnite. The olivine has almost completely altered to serpentine.

This rock is characterized by a clear banded structure of white and dark parts. The gabbro situated near Berong, however, does not show any banded structure.

A gabbro body located in detailed survey area B-1 trends N50°W, and dips 80°SW.

In area B-1, a troctolite layer underlies normal gabbro. Under the troctolite layer, a transitional zone and the cumulate dunite lies as cumulous phase of the Sultan Peak Gabbro.

5) Espina Basalt

The Espina Basalt is extensively distributed in the southern B-area, extending to the north up to the south of Berong on the west coast. It is also distributed in the areas to the south of Long Point in the west coast and to the northwest of Narra in the east coast.

It consists of basaltic pillow lava and diabase.

The basaltic pillow lava is gray to pale gray, and its pillow structure is clear. The size of the pillow ranges from 0.4m to 1.0m. Massive basalt is also observed. Boulders of red chert are found in the distribution area of the basalt. It is assumed that the chert is intercalated by the basaltic pillow lava.

The diabase is gray to pale gray, and shows the ophitic texture. It has undergone silicification in some cases. The basaltic pillow lava trends N30°W, and dips 40° west. The diabase dikes trend N20°W-N45°W, dips southwest.

6) Ransang Formation

The Ransang Formation is distributed in the small area on the west foot of the backbone mountains in the southern B-area.

It consists of micritic limestone containing a large amount of microfossils. It is said to be of Early Miocene age, and a part of it is correlated to the St. Paul Limestone of northern Palawan.

7) Isugod Formation

The Isugod Formation is distributed in lowland area around Berong on the west coast and the southwestern area. It mainly consists of shale and sandstone, accompanied with limestone.

8) Alfonso X III Formation

The Alfonso XIII Formation unconformably overlies the Espina Basalt near Aboabo in the southern B-area. It consists of coarse grained to muddy limestone and microcrystalline coral limestone. Judging from the nannofossil and foraminifera, it is probably of Late Miocene age.

9) Iwahig Formation

The Iwahig Formation conformably overlies the Inagauan Metamorphics and the Palawan Ophiolite in the lowland areas on the east coast of the B-area. It mainly consists of conglomerate and mudstone, accompanied with limestone in some places.

2-5-3 Geological structure

The geological structure of the B-area are ascribed to the emplacement of the ophiolite, which is believed to have generated during Late Cretaceous time and have thrust over the Panas Formation during the Eocene. The main features of the structure in this area are thrust fault, high angle fault, and folding.

1) Thrust Fault

It is presumed that two thrust faults exist in the B-area. One is on the bottom of the Mt. Beaufort Ultramafics, and the other is on the boundary between the green schist and amphibolite unit and quartz-mica schist and quartz schist unit of the Inagauan Metamorphics. Around the former, the harzburgite and dunite on the hanging wall side have undergone intense shearing and serpentinization, resulted mylonitization in some places. As for the latter, it has two different features. To the south of Berong, it borders the green schist/amphibolite and quartz-mica schist/quartz schist. In the Upper part of the Malasgao River and further north, it borders the Mt. Beaufort Ultramafics and quartz-mica schist/quartz schist. This means that the two thrust faults are situated between the Mt. Beaufort Ultramafics and Panas Formation. It lacks the green schist/amphibole facies in some places. The texture of the Mt. Beaufort Ultramafics generally trend NE to SW and dip southwest, therefore it is oblique to the general trend of the thrust faults.

The quartz-mica schist has been dated as 44.8 to 46.3 ± 6.8 Ma. It may be inferred that the thrust movement occurred in the Middle Eocene.

2) High Angle Fault

A high angle fault runs from the middle of the Batanbatan River in the central-southern area along the east coast in the B-area to the upstream area of the Tagbolante River on the west coast. This fault cut the Mt. Beaufort Ultramafics, and accompanies a sheared zone with 2m wide, in where intense serpentinization occurred. The fault trends N to S, and appears to be a left lateral fault on the geological map.

Other small scale faults exist in the middle of the Batanbatan River and along the Panacan River on the east coast, and the surrounding area of Berong and near Long Point on the west

coast.

3) Folding Structure

Folding structure exists in the area to the south of Berong, where the Inagauan Metamorphics are distributed. It shows repeatedly synclines and anticlines, and the general trend of the axes is NNE to SSW.

A lineation of orthopyroxene and other minerals exists in the Mt. Beaufort Ultramafics, but its orientation and dip varies area by area. It is assumed that there are folding structure in the banded structures, but details are not yet revealed.